Evolution of schooling propensity in the guppy drives changes in anti-predator behavior that are linked to neuroanatomy

Alberto Corral-Lopez*[1,2,3], Alexander Kotrschal[2,4], Alexander Szorkovszky[5,6], Maddi Garate-Olaizola[2,7], James Herbert-Read[8,9], Wouter van der Bijl[1], Maksym Romenskyy[6,10], Hong-Li Zeng[11,12], Severine Denise Buechel[2,4], Ada Fontrodona-Eslava[2,13], Kristian Pelckmans[12], Judith E. Mank[1], Niclas Kolm[2]

*corresponding author: corral@zoology.ubc.ca

Affiliations

1 - Department of Zoology, University of British Columbia, Vancouver, Canada
2 - Department of Zoology/Ethology, Stockholm University, Stockholm, Sweden.
3 - Division of Biosciences, University College London, London, United Kingdom
4 - Behavioural Ecology, Wageningen University & Research, Wageningen, Netherlands.
5 - RITMO Centre for Interdisciplinary Studies in Rhythm, Time and Motion, University of Oslo, Oslo, Norway
6 - Department of Mathematics, Uppsala University, Uppsala, Sweden.
7 - Department of Ecology and Genetics, Animal Ecology, Uppsala University, Sweden
8 - Department of Zoology, University of Cambridge, Cambridge, UK.
9 - Aquatic Ecology, Lund University, Lund, Sweden.
10 - Department of Life Sciences, Imperial College London, London, UK.
11 - School of Science, Nanjing University of Posts and Telecommunications, Nanjing, China.
12 - Department of Information Technology, Uppsala University, Uppsala, Sweden.
13 - Centre for Biological Diversity, School of Biology, University of St Andrews, St Andrews, UK

Abstract

One of the most spectacular displays of social behavior is the synchronized movements that many animal groups perform to travel, forage and escape from predators. However, the mechanistic basis of the evolution of such collective behaviors, as well as their fitness effects, remains empirically untested. Here, we study anti-predator behavior in guppies experimentally selected for divergence in polarization, an important behavioral aspect of coordinated movement. We find that groups from artificially selected lines remain more polarized than control groups in the presence of a threat. Neuroanatomical measurements show these behavioral differences are linked to changes in brain regions previously suggested as important regulators of perception, fear and attention, and motor response. We use further analyses of behavior and visual capabilities to show that differences in anti-predator behavior are not attributable to changes in visual perception, but likely to more efficient transfer of social information in polarization-selected fish. Our findings highlight that brain morphology may play a fundamental role in the evolution of coordinated movement and anti-predator behavior.

Introduction

Animals regularly gather - for safety, for exploiting resources, or for mating. Group-living often leads to spectacular forms of collective behavior, and individuals in many taxa coordinate their movements in order to increase efficiency in foraging and travelling, or to confuse predators [1]. To date, we have a detailed understanding of the interaction rules that produce highly coordinated movements in animal groups [e.g. 2,3], as well as the ecological factors that produce the broad variation observed across and within species[4]. Collective motion has evolved many times in fish, and is underpinned by the efficient acquisition of information through the sensory system, mainly through visual cues[5]. Fish schooling is widely understood as a behavioral adaptation to reduce the risk of predation[6]. But although correlation-based analyses have revealed how predation levels are associated with variation in collective motion in wild populations (see for instance [7]), the causal aspects are still unclear, particularly how evolutionary changes in collective motion contribute to anti-predator specific situations, or what type of visual information and information processing schooling fish use to identify and avoid predators as groups.

The brain, as the central organ controlling locomotion, sensory systems and decision-making, should play a major role in the ability to coordinate movements in animal groups. As such, variation in the anatomy of the brain could be an important mechanism behind the evolution of collective motion. Despite its potential importance, studies explicitly testing the role of neuroanatomy in collective motion are scarce. However, the link between social factors and changes in multiple brain structures across taxa is well established[8–11] (Barton 1996, Burish et al. 2004, Chee et al 2013, Triki et al. 2019).

This association is particularly well studied in fish, where approximately half of marine and freshwater species come together in groups at different life stages[12]. For instance, Tanganyikan cichlids species with more complex social structures have larger telencephali and hypothalami[13], both parts of the fish forebrain, a region with important function in social behavior [14], which has also been associated with social competence in cleaner fish and social orienting in zebrafish[10,15]. In addition, exposure to larger groups during development in nine-spined stickleback is correlated with larger size of another brain region, the optic tectum, the visual center in the fish brain [16].

Schooling requires sensory perception of neighbors' movements and positions and motor control to enact speed and directional changes. Brain regions associated with fish social behavior have also been implicated in the few studies explicitly testing the link between neuroanatomy and schooling behavior. First, lesion studies in goldfish (*Carassius auratus*) showed that individuals with ablated telencephalon exhibited reduced activity and association with conspecifics[17]. Second, a study on surface and cavefish populations of *Astyanax mexicanus* living in different light environments showed an underlying positive correlation between optic tectum size and schooling propensity differences between populations[18]. These limited studies highlight the potential role of neuroanatomy in schooling, as well as the need to account for environmental variation in analyses.

Here we use artificial selection lines of guppies (*Poecilia reticulata*) with divergence in schooling propensity, which offer a unique opportunity to empirically evaluate the link between evolution of general collective behavior, specific anti-predator behavior and neuroanatomy[19]. In relation to many fish species that associate in large schools, guppies have relatively low schooling propensity, with high levels of variation across individuals and across populations as a function of external

109 factors such as predation risk or food availability[20,21]. In our selection lines, intrinsic schooling
110 propensity was increased in female guppies by over 15% compared to controls in just three
111 generations by selecting individuals that exhibited higher polarization, the level of alignment
112 between individuals moving together in a group[19,22]. Previous assays in polarization-selected
113 females provided a good account of changes in their individual movement patterns in relation to
114 control females, including higher alignment and attraction to neighbors[19].
115
116 We use these lines to investigate potential changes in the visual system and anti-predator behavior
117 following directional selection for schooling propensity, as well as to study the association
118 between increased schooling propensity and changes in brain anatomy. For this, we first evaluated
119 collective motion patterns and predator inspection in groups of polarization-selected and control
120 female guppies, and found that polarization-selected females inspected threats for shorter times
121 and formed more cohesive groups when exposed to these threats than control females. Second, we
122 quantified brain region sizes with microcomputed tomography (microCT) and found that these
123 behavioral differences were linked to changes in brain regions previously suggested as important
124 regulators of perception, fear and attention, and motor responses. Third, we performed
125 comprehensive tests of visual capabilities, spanning morphological, visual acuity and temporal
126 resolution measurements, which revealed that despite the occurrence of significant changes in
127 brain regions regulating the visual system, the differences in schooling propensity and anti-
128 predator behavior between the selection lines do not appear to be driven by differences in the
129 capacity to acquire visual information. By linking changes in schooling propensity to function in
130 an ecologically relevant setting and to brain structure size variation we identify potential
131 evolutionary pathways leading to collective motion.
132
133
134 # Results
135
136 ## Collective motion in response to predation threat in guppies following artificial selection
137
138 We investigated whether selection for higher schooling propensity affected cohesiveness and how
139 individuals from groups react in response to neighbor movement in a predation context. These

behavioral decisions should have major fitness consequences in this species[23]. Specifically, we recorded and tracked fish in an experimental arena to obtain positional data and assessed collective motion of groups of eight guppies when exposed to an imminent threat, the presence of an artificial replica of a pike cichlid (*Crenicichla frenata*), a natural predator in wild populations of Trinidadian guppies. Furthermore, we exposed these groups to a non-predator-shaped object to allow for comparisons when presented to a novel object. These assays were performed in combination with open field tests (OFT's) on the same fish groups. Previous analyses of the data for OFT's in these groups provided evidence that selection for polarization altered individuals' speed, how individuals aligned with, and how individuals were attracted towards conspecifics during group motion[19].

Our analyses of collective motion of female groups exposed to a predator model and a novel object showed predictable results in relation to previous findings observed in OFT's. In the presence of a predator model or a novel object, we observed an overall strong decline in the polarization of the groups, as well as in individuals' speed (Supplementary Table 1, Fig. 1A). Differences between polarization-selected and control groups in these traits were still present, but to a reduced degree in the presence of these stimuli in the experimental arena (Supplementary Table 1, Fig. 1). Similarly, overall attraction towards conspecifics in female groups (using median nearest neighbor distance as proxy) was stronger when exposed to both stimuli than in OFT's. Yet, differences between polarization and control lines in nearest neighbor distance previously observed in OFT's[19], were no longer observed when these groups of fish were exposed to a predator model and a novel object (Fig. 1A; Supplementary Table 2). We observed no differences between the response towards the predator model compared to the novel object in how these stimuli altered the attraction towards conspecifics of these groups ($LMM_{attraction}$: novel object vs predator model: t= 0.331; df = 335; p = 0.941). On the contrary, the predator model elicited a stronger response than the novel object in the speed and polarization of the group. Specifically, collective motion data showed that guppy groups were slower and less aligned in the presence of a predator model ($LMM_{polarization}$: novel object vs predator model: t = 2.87; df = 338; p = 0.011; LMM_{speed}: novel object vs predator model: t = 4.71; df = 338; p < 0.001). Visual inspection of heatmaps summarizing data of group alignment in combination with positional data concords with these results obtained from statistical models using summary statistics for each group (Fig. 1B). Yet,

differences in polarization between control and polarization-selected groups in open field and novel object assays were consistent across all regions of the arena, while the observed statistical differences in assays with a predator model were more pronounced in positions further away from the head of the model (Fig. 1B).

Social information processing in response to predation threat

To characterize potential differences in how efficiently social information spreads in polarization-selected and control fish groups when exposed to a predator threat, we quantified inspection behavior of individuals in our groups of eight fish in the presence of a predator model, and collective motion of the group at times and in locations associated to predator inspection behavior during our assays.

Predator inspection behavior

We scored recorded videos for the start and end point for each predator inspection performed by one randomly selected fish in each video. Analyses of predator inspection data showed that females from control lines presented a higher tendency to inspect the predation threat presented in the experimental arena than polarization-selected females. Specifically, we observed that total time inspecting and the mean duration of predator inspections were significantly shorter in polarization-selected females ($GLMM_{time\_inspecting}$: selection: Ratio = 0.79 (0.66-0.95), t = -2.52, p = 0.011; $GLMM_{mean\_inspection}$: selection : Ratio = 0.82 (0.66-0.96), t = -2.49, p = 0.013, Fig. 2d-e, Supplementary Table 3), while the total number of inspections showed a similar trend ($GLMM_{inspections}$: selection: Ratio = 0.87 (0.75-1.01), t = -1.85, p = 0.064; Fig. 2c, Supplementary Table 3).

Collective motion during predator inspections

Analysis of positional data and median distance to the stimulus presented in our assays suggested that most inspection behaviors to the predator model were performed during the initial 3 minutes of the assays (Supplementary Figure 1). Further, the majority of inspections were performed at a range closer than 200 mm and in the tail area of the predator model presented in the experimental arena (Fig. 1A; Fig. 2A). Consequently, we filtered our data to evaluate collective motion patterns

of fish groups in the time and locations where predator inspections were performed during our assays (see methods). The overall differences in group polarization found between polarization-selected and control groups were maintained in areas within 200 mm of the predator model (Fig. 2B; $LMM_{polarization < 200mm - predator\ model}$: t = -1.984, df = 272, p = 0.048; Supplementary Table 4a-b). Inspection behavior is mainly performed from areas with reduced risk of attack from a predator. In line with such expectation, we found that polarization of all groups was greatly reduced in the area of the predator model tail (Fig. 2B). However, we found no differences in group polarization between selected and control females in the head area of the predator model, but a stronger maintenance of group polarization of polarization-selected females in close proximity to the tail of the predator model ($LMM_{polarization - head\ area}$: t = -1.53, df = 4.58, p = 0.190; $LMM_{polarization - tail\ area}$: t = -1.53, df = -3.48, p = 0.029; Fig. 2B, Supplementary Table 5a-b).

Changes in neuroanatomy following artificial selection

We used microcomputed tomography (micro-CT) to determine whether the volumes of 11 major brain regions and overall brain volume of female guppies might be associated with selection for higher schooling propensity and changes in collective behavior in response to predator threats. Specifically, we used micro-CT scans to reconstruct the brain anatomy of 13 polarization-selected females, and 15 control females (see methods). Polarization-selected and control fish showed no differences in whole brain volume in relation to their body size ($LMM_{wholebrain}$: t = -0.41, df = 23.29, p = 0.682; Fig. 3a). However, analyses of the volume of each region in relation to the rest of the brain indicated that the thalamus and optic tectum cups are larger in polarization-selected than control females ($LMM_{thalamus}$: selection: t = 2.187, df = 25, p = 0.038; $LMM_{o.tectum}$: selection: t = 2.409, df = 23.09, p = 0.024; Fig. 3a), and the medulla oblongata is larger in control females ($LMM_{medulla}$: selection: t = -2.65, df = 23.91, p = 0.013; Fig. 3a). All other eight brain regions measured presented no difference between polarization-selected and control females in relative volume (Fig. 3a-b, Supplementary Table 6).

In parallel, we analyzed brain region volume differences using a more conservative approach and found similar and consistent differences between selection lines. Specifically, we used a multivariate Bayesian model that included the relative size of the 11 brain regions as dependent

variables. Posterior samples drawn from the multivariate model indicated that confidence intervals for the difference in relative volume in the medulla oblongata, the optic tectum cups and the thalamus between polarization-selected and control females did not overlap with zero (Supplementary Table 7a).

We then used the multivariate Bayesian model to evaluate the correlation in relative brain region volume between multiple regions measured. We focused on evaluating correlations with other brain regions for the three regions significantly differentiated between lines following artificial selection (Supplementary Table 7b). We found no correlation between optic tectum cup relative volume and volume of any other region measured. However, we found a significant inverse correlation between thalamus and medulla relative volume ($rescorr_{Medulla\text{-}Thalamus}$: -0.40 ± 0.14; lower/upper 95% CI: -0.65 / -0.12). This finding suggests that the opposite differences observed in the volume of these two brain regions between control and polarization-selected female guppies may be linked to changes in brain development processes associated with artificial selection for higher coordinated motion.

Information acquisition through the visual system

Efficiently acquiring information through the sensory system, mainly through visual cues, is a basic principle of collective motion in shoaling fish[5]. Given observed differences in the size of the optic tectum cups between polarization-selected and control fish, we investigated potential differences in visual perception between lines. For this, we compared eye morphology and two key characteristics of the visual system to track movement of conspecifics, visual acuity and temporal resolution.

Eye morphology

We quantified eye morphology in a total of 112 individuals from polarization-selected and control lines. Eye size is a common indicator of visual capacities of organisms[24], and comparative studies across fish species suggest that larger eyes correlate with improved visual abilities[25]. In our study, we found no difference between the lines in either absolute eye size or relative eye size, the proportional size of the eye in relation to body size (Fig. 4A; $LMM_{eye\ size}$: selection: t = -0.52, df = 2, p = 0.658; $LMM_{relative\ eye\ size}$: selection: t = -0.13, df = 2, p = 0.906; Supplementary Table 8).

Visual acuity

We further assessed potential differences in visual perception between selection and control lines by quantifying visual acuity in the same individuals for which eye morphology was measured. Visual acuity allows an individual to resolve spatial detail and can be critical for an organism's fitness[26]. We measured visual acuity in our fish by quantifying their innate optomotor response in contrasting rotating gratings. This a widely used method to study visual acuity in multiple fish species, including guppies[27–29], and we have previously used this approach to evaluate the visual system of guppies in similar contexts[30,31]. Following the methods in ([30]), we exposed our fish to a series of six stimuli with rotating and static gratings of different widths at the lower end of the known guppy visual acuity, where thinner widths are more difficult to perceive. When comparing optomotor response between polarization-selected and control fish, we found no difference in their average optomotor response combining data from all stimuli (LMM_{acuity}: selection: $t = 0.11$, $df = 12.88$, $p = 0.913$; Supplementary Table S9a), or in analyses independently evaluating specific optomotor response for any of the 6 stimuli presented (Fig. 4B; Supplementary Table 9c).

Visual resolution tracking movement

Although the ability to resolve spatial detail, acuity, is arguably an important visual parameter for guppies to recognize conspecific positions in shoals, it provides no information on an individual's ability to track movement[32]. Similar to many social fish species, guppies swim with a saltatory movement style that features discrete changes in speed and direction[7]. Consequently, we implemented an additional experiment that evaluated potential differences between polarization-selected and control fish in their temporal assessment of speed and direction changes. Using the same experimental apparatus used to evaluate visual acuity, we video recorded female guppies from our selection and control lines when they were exposed to a single-width rotating stimulus (see methods). We next used automated tracking to obtain orientation and speed of the fish for each frame and to quantify their direction and speed in relation to the stimuli presented at each time point.

Overall, fish followed the direction of the rotating stimulus for a significant proportion of the time. This was the case when the stimuli were presented in both a clockwise direction an in

counterclockwise direction (Supplementary Figure 2, Supplementary Table 10). Overall, swimming speed did not significantly deviate from the stimuli rotating speed at the two lowest speed levels (Supplementary Figure 2, Supplementary Table 10), but was less than the stimuli speed at the two highest speed levels (Supplementary Figure 2, Supplementary Table 10). This was true for both directions in which stimuli were presented, but the mismatch between swimming and stimuli rotation speed was greater at the higher speed when the stimulus rotated anticlockwise (Supplementary Figure 2, Supplementary Table 10).

We compared the performance of polarization-selected and control fish in the test to evaluate their visual temporal resolution while shoaling. We found no differences between selection and control lines in their deviation of their swimming speed in relation to the stimuli rotating speed for their combined scores across speeds and direction of rotation (Fig. 4C; $LMM_{speed\_deviation}$: selection: $t = -0.46$, $df = 2.64$, $p = 0.863$; Supplementary Table 10a), or for their speed observed at any particular speed at direction of rotation (Supplementary Figure 2, Supplementary Table 10a). Similarly, polarization-selected and control females spent similar proportions of time following the stimuli during changes in stimuli rotating speed (Supplementary Figure 2; Supplementary Table 10a; $LMM_{proportion\_time}$: selection: $t = 0.10$, $df = 2.52$, $p = 0.928$).

Discussion

Our work demonstrates that selection for schooling behavior in female guppies has important implications for anti-predator responses in this species. Analyses of motion patterns in these fish shows that polarization-selected groups maintain higher activity and sociability when exposed to a potential predator threat. In addition, our analyses suggest that individuals from polarization-selected groups rely more on neighbor information during a predator threat, as they spent less time inspecting individually. We further studied visual capacities in these fish and found no differences between polarization-selected and control fish, suggesting that the differences in collective motion and predator inspection behavior observed are not driven by their ability to distinguish the threat at longer distances or to visually acquire information on neighbor movements.

In parallel, our results suggest that artificial selection for higher schooling propensity has produced significant changes in the brain anatomy of female guppies. Neuroanatomical measurements indicate that polarization-selected fish exhibit a larger thalamus and a large optic tectum cup, but a smaller medulla oblongata, compared to control fish. These rapid changes in brain region sizes in response to selection for polarization behavior are consistent with previous artificial selection directly on neuroanatomy, which resulted in rapid shifts in both relative brain size and relative telencephalon size, in just a few generations in guppies[33,34].

Below, we discuss the implications of these discoveries for our understanding on how the association between brain morphology and anti-predator behavior might drive the evolution of collective behavior.

Information processing in a predation threat context

Our behavioral analyses indicate that rapid evolution of schooling propensity affects how groups of fish behave when encountering a threat. Fish schooling is widely understood as a behavioral adaptation to escape the effect of predation[1]. These synchronized movements have been shown to confer two major benefits to fish schools, facilitating escape through transfer of information from closer neighbors[35], or by confusing the predator in which individual to attack[36]. The use of a static predator model in our assays does not allow us to infer any potential benefit of higher schooling propensity on the confusion effect towards predators. However, our results show that directional selection and associated changes in the brain lead to robust behavioral changes across multiple contexts and that it might affect individual ability to efficiently process social information in response to predation. The reduced time spent inspecting the predator model by polarization-selected females, coupled with the fact that polarization-selected groups remained more aligned closer to the predator model, especially around the tail of the predator, suggest this a likely possibility. However, further comparisons within asocial and social contexts should be implemented to disregard the alternative explanation that directional selection leads to changes in predator inspection behavior also when fish have no access to social information.

Our study only measured fitness effects indirectly, using a predator model, following directional selection for polarization. Yet, previous work demonstrated that shorter inspection times towards

the same predator models are associated with higher survival in the species[37,38]. Given our findings, this is likely an important fitness benefit for individuals showing higher coordination with conspecifics. This benefit might trade-off with a reduced level of private information from potential threats obtained by these individuals. These factors are arguably important selective pressures in natural populations where guppies from high predation habitats swim with higher coordination and in larger groups[39,40]. Indeed, guppies from higher predation populations have been shown to rely more on social information for foraging resources, than those from lower predation populations[41]. This is similar in the three-spined stickleback (*Gasterosteus aculeatus*), where the transfer of information between conspecifics was more effective in more polarized groups[42]. Further studies evaluating fitness effects of relying in social versus individual information across different predation pressures is paramount to understand how anti-predator behavior and collective motion drive evolutionary patterns at the proximate level.

In addition, across all tests performed we consistently found higher activity in polarization-selected females. Previous assays in these fish evaluating maximal speed and endurance ruled out the possibility that differences in collective motion patterns observed between polarization-selected and control fish were driven by motor capacities[19]. In fact, activity is primarily associated with the exchange of directional information according to a previous analysis of collective motion patterns in guppies[39]. The difference in activity detected in our study may suggests that there are differences in the selection lines in their ability to detect neighbor movements, or even to detect the threat itself. Indeed, synchronized movements require an accurate detection and representation of the near and far field of view around an individual to orient the body and maneuver accurately in reaction to fast neighbor movements[5]. While this could possibly be due to differences we observe in the primary visual center of the fish brain (the optic tectum), our morphological and physiological tests performed to evaluate visual capacity indicate the opposite. Moreover, our previous work using the same methods on brain size selection lines in guppies[30] indicates that differences observed between polarization-selected and control females are not due to differences in the acquisition of visual information. Rather, the combination of neuroanatomical, behavioral and physiological data from our study suggests that in a predation context, effective decision-making based on social information and effective processing of visual information to synchronize swimming with close neighbors are central for the observed differences in anti-predator behavior.

Brain morphology and collective behavior

The study of brain anatomy in artificially selected fish allows to study brain function in relation to behaviors that have important implications in the evolution of sociality. In our study, we found two brain regions that were larger in relation to the rest of the brain in polarization-selected fish, the optic tectum cup and the thalamus. The optic tectum is the terminus of a vast majority of optic nerve fibers and axons of retinal cells[43] and as such is the primary vertebrate visual center. Despite wide variation in optic tectum size across teleost species, this region functions to form instant representations of the immediate surroundings[43]. This function is primarily achieved in superficial layers of the tectum[44], which corresponds to the optic tectum cup region used in our neuroanatomical parcellation of major brain regions in the guppy[45].

The evolved differences in optic tectum cup size between polarization-selected and control female guppies we found are concordant with phenotypic plasticity findings in nine-spined stickleback where it was found that individuals reared in groups developed larger optic tectum that those reared individually[16]. Differences in the ability to acquire sensory input have previously been associated with differences in schooling propensity[46]. In our experiment, rapid evolution of higher schooling did not lead to changes in visual perception or eye morphology. Together, these findings suggest that differences found between polarization-selected and control lines in this section of the optic tectum should have an effect in their ability to process visual information in order to control body orientation during complex social maneuvers, but not in sensory information acquisition. This is consistent with the role of the optic tectum in information processing in relation to the telencephalon, a region of the brain commonly associated with decision-making in relation to social behavior. Specifically, representation of the immediate surrounding in the optic tectum is self-centered while the representation is allocentric in the telencephalon[43]. This self-centered representation leads to important visuomotor computations of stimuli and can have important roles in eye and body orienting as well as in predator evasion[47].

The thalamus was also enlarged in female guppies following artificial selection for higher coordinated motion. While mostly studied in mammals, it seems that the thalamus plays prominent roles in regulating attention and alertness and motor control through the modification, filtering and

distribution of sensory information into decision-making regions of the brain[48,49]. Recent findings suggest similar functionality between homologous region of the mammalian and teleost brain as defined in zebrafish as the *wider thalamus* region[48], and comparable to the guppy thalamic region parcellated in our measurements. Specifically, the zebrafish thalamic region acts as the origin of the main inhibitory neurons in the central nervous system (GABAergic neurons)[50], with an important role in attenuating aggressiveness and the response to fear[51,52]. Our findings in anti-predator behavior assays are consistent with functional convergence between the mammalian and fish thalamic regions. The shorter time spent inspecting a predator threat observed in polarization-selected fish (with larger thalamus) is likely explained by better ability to regulate alertness and fear response towards a potential threat. While not directly addressed in this study, the regulatory role of the thalamus in aggressiveness is concordant with common expectations of lower aggression levels in group-living species (reviewed by [53]). As such, further quantifications of the anatomical characteristics of the thalamus in relation to aggression levels within and across species is a promising avenue for future research.

In contrast to the thalamus and the optic tectum cup, we found that the medulla oblongata was smaller in polarization-selected lines. Consistent with this, in larval coral reef fishes, the inferior and vagal lobes, which are subregions of the medulla, are larger in solitary as compared to more social species[54]. The medulla oblongata is an important relay center of nervous signals between the spinal cord and ascendant brain regions and has three core functions in teleosts. First, the medulla oblongata functions in motor control through the presence of efferent motor neurons that relay signals to the cerebellum[55]. Despite this function, we find no differences in motor control capabilities between polarization-selected and control female guppies[19,56]. The medulla oblongata also controls anti-predator responses through neuron firing in two large neurons present in this region, the Mauthner-cells[57]. Interestingly, a previous study found that grouping reduces the frequency of startle behavior, commonly observed in combination with predator inspections[58]. These findings are consistent with the reduction of predator inspection behavior we observed in fish with higher schooling propensity. Finally, the medulla has a central function the processing of somatosensory signals, with special emphasis in auditory and gustatory signals[59,60]. While not tested in this study, it may be that the reduction in medulla observed in polarization-selected lines might be associated with important changes in the auditory system and the ability to perceive

different tastes. In line with this reduction in the size of the medulla oblongata, our results show that three other brain regions have significant hypoallometric relationships with the medulla (see Supplementary Table 4b): the cerebellum (motor control center), the thalamus and the hypothalamus (hormonal regulation center). Gene expression of *angiopoietin*-1, a locus implicated in brain tissue development, showed contrasting expression levels between the medulla and the thalamic and hypothalamic regions[61]. Based on this, we hypothesize that selection for more coordinated motion leads to a trade-off between general sensory capabilities that are not important in coordinated movements and specific sensory capabilities required to coordinate movement with neighbors.

Unlike the auditory and taste systems, the mechanosensory system (lateral line) is important for schooling through cues that allow fish to assess neighbor changes in speed and direction[62], although this is more critical in low light and high turbidity conditions, which are very different to our experiments[6]. In the future, it will be interesting to investigate the association between schooling propensity, brain anatomy and potential trade-offs between sensory and mechanosensory capacities.

Conclusion

Our empirical approach with behavioral assays on artificial selection lines with divergence in polarization show that collective motion differences are consistent in the presence of a predator threat and that predator inspection behaviour varies between the selection lines and the control lines. Moreover, we reveal differences in neuroanatomy that could provide a mechanistic explanation to the observed behavioural differences. Based on our discoveries, we propose that changes in behavior are intimately intertwined with matching changes in brain morphology during the evolution of collective behavior.

Methods

Artificial selection for schooling propensity

We evaluated the association between brain anatomy and collective motion in female guppies following artificial selection for higher polarization. Extensive detail on the selection procedure can be found in ([19]). In short, groups of female guppies were tested in repeated open field tests and sorted in relation to the mean polarization of the group, the degree to which the individuals of a group move with higher alignment[19,22,63]. For three generations, females from groups with higher polarization were bred with males from those cohorts to generate three up-selected polarization lines. In parallel, random females were exposed to the same experimental conditions and bred with unselected males to generate three control lines. Third generation polarization-selected females presented on average a 15% higher polarization and 10% higher group cohesiveness (i.e. 10% shorter nearest neighbor distances) than control females[19]. The selection procedure targeted polarization on female groups and we found a weaker response to selection in males, and therefore subsequent neuroanatomical, behavioral and physiological studies focused on females. All fish were removed from their parental tanks after birth, separated by sex at the first onset of sexual maturation, and afterwards kept in single-sex groups of eight individuals in 7 L tanks containing 2 cm of gravel with continuously aerated water, a biological filter, and plants for environmental enrichment. We allowed for visual contact between the tanks. The laboratory was maintained at 26°C with a 12-h light:12-h dark schedule. Fish were fed a diet of flake food and freshly hatched brine shrimp daily.

Anti-predator response in guppies following artificial selection

Collective motion

We evaluated anti-predator behavior in polarization-selected and control female guppies by conducting assays on 164 groups of eight fish in white arenas with 55 cm diameter and 3 cm water depth. Each group was initially assessed in an open field assay in the arena for 10 minutes, and collective motion data from these open field assays was previously used to analyze differences in social interactions[19]. After 10 minutes, we sequentially introduced a novel object and a predator model for 6-minute periods in the centre of the experimental arena. In half the assays, we introduced the novel object first and the predator model second, with the order reversed in the other half of the assays. We used a blue coffee mug as a novel object and a fishing lure custom-

painted to resemble the pike cichlid *Crenicichla frenata*, a natural predator on the guppy, as the predator model. These objects have been previously used to successfully reproduce natural behaviors of the guppy in response to a novel object and a predation threat[38]. Prior to the start of the assay, the eight-fish group was confined in the centre of the arena for two minutes in an opaque white 15 cm PVC cylinder. After this acclimation period, we lifted the cylinder and filmed the arena using a Point Grey Grasshopper 3 camera (FLIR Systems; resolution, 2048 pixels by 2048 pixels; frame rate, 25 Hz).

We tracked the movement of fish groups in the collected video recordings using IDTracker[64] and used fine-grained tracking data to calculate activity, polarization and attraction in Matlab 2020 following methods established in ([65]). These three variables characterize the two main axes of collective motion in guppies, activity (speed) and sociability (polarization and attraction)[39]. For activity, we calculated the median speed across all group members and frames in each assay. For group polarization, we calculated the median global alignment, which indicates the angular alignment of all fish in the arena. Calculations of median global alignment only considered frames in which at least six individuals formed a connected group, with an interindividual distance of less than 10cm counting as a connection. For attraction, we obtained the median distance to the nearest neighbor for every fish across all frames. For all variables, we disregarded tracking data that did not present a minimum of 16 consecutive tracked frames. To estimate the effect of the predator model and novel object on group collective motion patterns, we additionally calculated group polarization across all frames that contained reliable data for every group. We then generated a heatmap with average values across polarization-selected and control groups that occurred within 20 x 20 mm grid cells (Fig. 1B). We used the centroid of the group to estimate group position within the arena. Grid cells that did not contain values for a minimum of 8 groups per treatment were disregarded. To evenly compare motion patterns when presented with a novel object and a predator model to those obtained during the open field assays, we limited our analysis of the open field assay data to the initial six minutes of the recording.

We used LMMs with median speed, polarization and attraction as dependent variables to test for potential differences between polarization-selected and control lines. Selection regime, the type of stimulus presented and the interaction between these two were included as fixed effects, and

543 body size of fish was coded as a covariate, with a random intercept for each replicated selection
544 line and the order of presentation of stimuli as random factors. All models were run in R
545 (v.4.1.3) using lme4 and lmerTest packages[66,67]. Model diagnostics showed that residual
546 distributions were roughly normal with no evidence of heteroscedasticity. We obtained post-hoc
547 comparisons of the response between selection line regimes at different levels of other fixed
548 effects in the previous models using the emmeans package[68] with the tukey-adjustment method
549 for multiple comparisons.
550
551 *Predator inspection behavior*
552 ***Behavioral scoring.*** Positional data and analyses of median distance to center in our data indicated
553 that groups of fish swam closer to the stimuli presented in the initial minutes following the addition
554 of a predator model in the experimental arena, when compared to the same time periods following
555 the addition of a novel object (Fig. 1A; Fig. 2A; Supplementary Figure 1). This observation
556 matched previous findings in similar experiments performed on guppies[38] and likely corresponds
557 to the stereotypical behavioral response of guppies to inspect and gain information of a potential
558 threat[23]. A predator inspection in guppies is characterized by an approach to the predator,
559 monitoring predator activity and swimming sideways with an arched body. Based on this
560 information, we manually visualized the videos during the first three minutes after addition of the
561 predator model and scored the behavior of one randomly selected fish in the group using BORIS[69].
562 While blind to the selection line treatment, the start and end time of each predator inspection
563 performed by the focal fish was scored for each video. We used the start and end time of predator
564 inspections to calculate the number of inspections, average inspection duration and the total time
565 that was spent inspecting per fish. Next, we fit a statistical model for each variable as a dependent
566 variable using a zero-inflated beta distribution and a logit link function for the conditional mean
567 in the package glmmTMb[70]. We used the selection line regime as a fixed effect. A random intercept
568 for each replicated selection line, and the order of presentation of the stimuli in the arena were
569 included as random factors in the model. We evaluated the adequacy of our fitted model using
570 scaled-residuals quantile-quantile plots, residual versus predicted values plots and a zero-inflation
571 test in the DHARMa package[71].
572

Group collective motion during predator inspections. We analysed positional data for each group by binning the observations in a grid, with cells being 20 x 20 mm. For each trial, we calculated a density map, where the value for each grid cell was the fraction of all observations that occurred within that cell. The resulting density maps are a normalized representation on how often each grid cell was visited by individuals in our groups of 8 fish when exposed to different stimuli (Fig. 2A). We used information from positional data to calculate summary statistics in different areas of interest. Predator model assays presented unique spatial patterns in areas closer to the stimulus presented, with higher densities in the tail area of the predator model (Fig. 2A). Based on these factors, we calculated two new summary variables for each group: i) median polarization of the group when the average position of the group was closer than 200 mm for predator model and novel object assays; and ii) median polarization of the group in locations closer to the head (y-position > 0) and the tail (y-position < 0) in predator model assays. We used LMMs with these new calculated variables as dependent variables in the model to test for potential differences between polarization-selected and control lines. Selection regime, the type of stimulus presented or location in the tank were included as fixed effects, with a random intercept for each replicated selection line and the order of presentation of stimuli as random factors. All models were run in R (v.4.1.3) using lme4 and lmerTest packages[66,67]. Model diagnostics showed that residual distributions were roughly normal with no evidence of heteroscedasticity. We obtained post-hoc comparisons of the response between selection line regimes at different levels of other fixed effects in the previous models using the emmeans package[68] with the tukey-adjustment method for multiple comparisons.

Brain morphology of female guppies following artificial selection

We assessed neuroanatomical features of 15 polarization-selected and 15 control F3 fully-grown females (6 months old), divided equally across polarization-selected and control lines. We used microcomputed tomography (microCT, Skyscan 1172, Bruker microCT, Kontich, Belgium), and reconstructed cross-sections from scanned images following a protocol successfully implemented in a previous study evaluating neuroanatomical differences between guppies artificially up- and down-selected for relative brain size[45]. This protocol allowed us to obtain measurements of whole

brain size volume and relative brain region volume in 11 major brain regions in the guppy brain: olfactory bulbs, ventral telencephalon, dorsal telencephalon, thalamus, hypothalamus, nucleus glomerulus, torus semicircularis, optic tectum cup, central optic tectum, cerebellum, and medulla oblongata (Fig. 3B). Extended details on guppy brain region reconstruction from digital images can be found in ([45]). Two brains from polarization-selected lines were damaged during the protocol, which reduced the sample size to 28 samples. We tested for overall differences in whole brain size between polarization-selected and control lines using a linear mixed model (LMM) with brain volume as dependent variable, body size (standard length) as covariate, selection regime as fixed effect, and replicate as random effect. For the brain regions, we used two different approaches to determine whether selected and control lines differ in neuroanatomical features. First, we ran 11 independent LMMs with each region's volume as dependent variable, whole brain volume (excluding volume of the region of interest) as covariate, selection regime as fixed effect, and replicate as random effect. LMMs were run in R (v 4.1.3) using lme4 and lmerTest packages[66,67]. Second, to take into consideration that brain region volumes may be interdependent, we used a more conservative approach and analyzed the data using a Bayesian multilevel model that included 11 brain regions as dependent variables in a fully multivariate context. The full model included an analogous structure to those used in the independent LMMs for each brain region. Parameter values were estimated using the brms interface[72,73] to the probabilistic programming language Stan[74]. We used default prior distributions with student-t distribution (3, 0, 2.5) for all parameters. The model estimated residual correlations among all brain region volumes with a Lewandowski-Kurowicka-Joe (LKJ) prior with $\eta = 1$, which is uniform over the range −1 to 1. Posterior distributions were obtained using Stan's no-U-turn HMC with six independent Markov chains of 4000 iterations, discarding the first 2000 iterations per chain as warm-up and resulting in 12000 posterior samples overall. Convergence of the six chains and sufficient sampling of posterior distributions were confirmed by a scale reduction factor below 1.01, and an effective size of at least 10% of the number of iterations. For each model, posterior samples were summarized on the basis of the Bayesian point estimate (median), SE (median absolute deviation), and posterior uncertainty intervals by HDIs,

Visual information processing in response to predation threat

Visual acuity

We evaluated the ability to perceive detail (visual acuity) in 9-12 months old female guppies (59 polarization-selected, 57 control individuals) by assessing their optomotor response, an innate orient behavior induced by whole-field visual stimulation[75]. Briefly, we projected a video recording with rotating vertical black and white bands of six different widths (stimuli) on the walls of a white ring-shaped arena of 25/50 cm of inner/outer diameter. Previous optimization of the methods found that the use of these stimuli allowed us to evaluate the optomotor response at the lower end of the species' acuity[30]. We placed individual fish in between the inner wall of the arena and a transparent ring of 40 cm diameter. After a 2-min acclimation period, we recorded their response towards 6 different rotating stimuli and the static images of these stimuli using a Sony Cam HDR-DR11E recorder. Each stimulus was presented for 1 minute in random order. Extended methods and the optimization procedure for the stimuli used here can be found in ([30]). We manually scored the videos, recording the time that fish spent circling in the direction of the stimuli (clockwise) at a constant moving pattern using BORIS[69]. Behavioral scoring was performed blind to the treatment since only running numbers identified recordings. Likewise, scoring was blind to the rotation and bandwidth of the stripes since only the fish, but not the rotating stimuli, were visible during scoring. From the scoring, we calculated the proportion of time that a fish spent swimming in the direction of rotation of the stimuli, out of the total time that the different vertical black and white bands were presented to them.

Temporal resolution

Two weeks after visual acuity tests were completed in all fish, we measured the ability to track movement stimuli of different speeds (temporal resolution) in the same females from the polarization-selected (n = 58) and control lines (n= 55). We did not keep track of fish identity as fish were kept in groups with conspecifics of the same selection line and replicate between experiments. To evaluate temporal resolution, we placed fish in a white arena (50 cm diameter, 4 cm water depth) and exposed them to a projection of black and white bands of 3.5 cm width rotating clockwise and counterclockwise at four different angular speeds (14.4, 25, 36 and 45 degrees/sec). The movement of each individual was recorded for a total of 1380 seconds with a Sony Cam HDR-DR11E; a 300 seconds acclimation period and 1080 seconds of clockwise and counterclockwise rotations of a projection with black and white bands at multiple speeds.

Specifically, during each individual test, the 8 stimulus combinations (4 speeds, 2 directions) were presented separately five independent times for 23 sec. The total time of each individual test was 920 sec (23 sec per stimulus x 5 times during the test x 8 stimulus combinations). We randomized the order of presentation of different stimuli a priori, but this order was consistent for all fish. The stimulus changed speed with smooth transitions of 3 sec, accelerating or decelerating to the next speed.

To quantify speed and direction changes of fish in our experimental setup, we automated behavioral scoring and obtained positional data using the Loopy Deep Learning Module (Loopbio 2020) in MATLAB (v. 2020a). X and y coordinates were transformed into a polar coordinate system centered on 0 and estimated from positional data. We calculated fish orientation by taking the difference in the fish's position between frames and defined their relative orientation (with respect to the arena) with the arcsin ($\sin(\theta - \vartheta)$), where θ was the orientation of the fish and ϑ is the angle of the arena radius going through the fish position. Positive values represent a fish swimming clockwise around the arena, while negative values represent swimming counterclockwise. For each frame, we identified whether the fish was swimming in the same direction of the stimulus projected and calculated the total proportion of time swimming in the direction of the stimulus. We also calculated the speed (in degrees per second) of the fish at each frame by using the dot product of the positional vector between consecutive frames. Using these values, we calculated for each individual the average total speed for each of the stimuli presented, and the average speed deviation between the speed of the stimulus presented and the speed of the fish.

Eye morphology

After the temporal resolution experiments were completed, we measured eye morphology in the females from polarization-selected lines (n = 57) and control lines (n =55) that were previously assessed for visual acuity and temporal resolution. For morphological measurements, we anesthetized fish with 0.2 mg/l of benzocaine and took pictures of their left side. We measured eye diameter and body length in these pictures using ImageJ[76]. Relative eye size was calculated as the ratio of these two variables. Image analyses were performed by a single scorer who was blind to the selection line treatment in the photographs.

Statistics

We analyzed potential differences in optomotor response, temporal resolution and eye morphology between polarization-selected and control females using LMM's. For the visual acuity trials, the proportion of time rotating was the dependent variable of the model. Fixed effects included selection line regime and bandwidth of the rotating stimuli. To account for differences in activity between fish, we used the proportion of time moving when presented with a static image of the stimuli as a covariate in the model. A random intercept for each replicated selection line, identity of the fish, and an observation-level variable were included as random factors in the model. For temporal resolution, we used selection line regime, the speed of rotation and the direction of rotation as fixed effects. The full model included the interaction between the selection regime with both speed and direction of rotation. This model included the identity of the fish, and a random intercept for each replicated selection line as random factors.

For eye morphology, eye diameter and relative eye size were dependent variables and models included selection regime as a fixed effect and a random intercept for each replicated selection line as a random factor. Model diagnostics showed that residual distributions were roughly normal with no signs of heteroscedasticity in optomotor response and eye morphology analyses. Model diagnostics on both models for temporal resolution analyses indicated unequal residual variance across the range of predicted values and a potential unequal influence of outliers. While estimates in linear mixed-effects models (LMMs) are argued to be robust to violations of such assumptions[77], we used the robustlmm package in R (Koller 2016) to compare the estimates obtained with LMM's to robust models with the same predictors that provide reduced weights to outliers in the data[78]. Results were consistent regarding the modelling approach (Supplementary Table 11). We obtained post-hoc comparisons of the response between selection line regimes at different levels of other fixed effects in the previous models using the emmeans package in R[68] with the tukey-adjustment method for multiple comparisons.

Acknowledgements

We thank David Sumpter for important contributions to the conceptualization of the artificial selection procedure. We thank A. Rennie, E. Trejo, M. Amcoff and A. Boussard for help with fish husbandry. **Funding**: This work was supported by the Knut and Alice Wallenberg Foundation (102 2013.0072 to D.S., N.K., and K.P.), the Canada 150 Research Chair Program, and the European Research Council (680951 to J.E.M), the Swedish Research Council (2016-03435 to N.K., 2017-04957 to A.K., and 2018-04076 to J.H.-R.), and the Whitten Lectureship in Marine Biology, University of Cambridge (to J.H.-R.). **Author contributions**: N.K., K.P and J.E.M. contributed to conceptualization and funding acquisition of the project. A.K., A.S., M.R., S.D.B., J.H.-R., H.Z., K.P., and N.K. contributed to the design of the selection procedure. A.C.L, A.K., A.S., A.F.E., L.S.A, M.R., S.D.B. conducted research to obtain collective behavior data and predator inspection data. A.K. H.L.Z. and K.P. conducted research to obtain neuroanatomical data. A.C-L., M.G-O, and J.H-R. conducted research to obtain visual capacities data. A. C-L and W.vdB. performed formal analyses and visualization. A.C-L., J.E.M, and N.K. wrote the original draft. All authors contributed to the final version of the manuscript. **Competing interests**: The authors declare that they have no competing interests. **Data and materials availability**: All data and code needed to evaluate the conclusions in the paper will be deposited in an online repository. Additional data related to this paper may be requested from the authors.

References

1. Krause, J. & Ruxton, G. D. *Living in Groups*. (Oxford University press, 2002).
2. Couzin, I. D., Krause, J., Franks, N. R. & Levin, S. A. Effective leadership and decision-making in animal groups on the move. *Nature* **433**, 513–516 (2005).
3. Jolles, J. W., Boogert, N. J., Sridhar, V. H., Couzin, I. D. & Manica, A. Consistent Individual Differences Drive Collective Behavior and Group Functioning of Schooling Fish. *Current Biology* **27**, (2017).
4. Parrish, J. K. & Edelstein-Keshet, L. Complexity, Pattern, and Evolutionary Trade-Offs in Animal Aggregation. *Science (1979)* **284**, 99–101 (1999).
5. Strandburg-Peshkin, A. *et al.* Visual sensory networks and effective information transfer in animal groups. *Current biology* **23**, R711 (2013).
6. Pitcher, T. J. Functions of Shoaling Behaviour in Teleosts. in *The Behaviour of Teleost Fishes* (ed. Pitcher T. J.) 294–337 (Springer, Boston, MA, 1986).
7. Herbert-Read, J. E. *et al.* How predation shapes the social interaction rules of shoaling fish. *Proceedings of the Royal Society B: Biological Sciences* **284**, 20171126 (2017).
8. Barton, R. A. Neocortex size and behavioural ecology in primates. *Proceedings of the Royal Society B: Biological Sciences* **263**, 173–177 (1996).

9. Burish, M. J., Kueh, H. Y. & Wang, S. S. H. Brain Architecture and Social Complexity in Modern and Ancient Birds. *Brain Behav Evol* **63**, 107–124 (2004).
10. Triki, Z., Levorato, E., McNeely, W., Marshall, J. & Bshary, R. Population densities predict forebrain size variation in the cleaner fish Labroides dimidiatus. *Proceedings of the Royal Society B* **286**, 20192108 (2019).
11. Chee, S. S. A. *et al.* Social status, breeding state, and GnRH soma size in convict cichlids (Cryptoheros nigrofasciatus). *Behavioural Brain Research* **237**, 318–324 (2013).
12. Shaw, E. Schooling Fishes: The school, a truly egalitarian form of organization in which all members of the group are alike in influence, offers substantial benefits to its participants . *Am Sci* **2**, 166–175 (1978).
13. Pollen, A. A. *et al.* Environmental complexity and social organization sculpt the brain in Lake Tanganyikan cichlid fish. *Brain Behav Evol* **70**, 21–39 (2007).
14. O'Connell, L. A. & Hofmann, H. A. Genes, hormones, and circuits: An integrative approach to study the evolution of social behavior. *Front Neuroendocrinol* **32**, 320–335 (2011).
15. Stednitz, S. J. *et al.* Forebrain Control of Behaviorally Driven Social Orienting in Zebrafish. *Current biology* **28**, 2445-2451.e3 (2018).
16. Gonda, A., Herczeg, G. & Merilä, J. Habitat-dependent and -independent plastic responses to social environment in the nine-spined stickleback (Pungitius pungitius) brain. *Proceedings of the Royal Society B: Biological Sciences* **276**, 2085–2092 (2009).
17. Shinozuka, K. & Watanabe, S. Effects of telencephalic ablation on shoaling behavior in goldfish. *Physiol Behav* **81**, 141–148 (2004).
18. Loomis, C. *et al.* An Adult Brain Atlas Reveals Broad Neuroanatomical Changes in Independently Evolved Populations of Mexican Cavefish. *Front Neuroanat* **13**, 88 (2019).
19. Kotrschal, A. *et al.* Rapid evolution of coordinated and collective movement in response to artificial selection. *Sci Adv* **6**, eaba3148 (2020).
20. Magurran Anne E. *Evolutionary Ecology: The Trinidadian Guppy*. (Oxford University Press, 2005).
21. Bierbach, D. *et al.* Using a robotic fish to investigate individual differences in social responsiveness in the guppy. *R Soc Open Sci* **5**, 181026 (2018).
22. Szorkovszky, A. *et al.* Assortative interactions revealed by sorting of animal groups. *Anim Behav* **142**, 165–179 (2018).
23. Dugatkin, L. A. & Godin, J. G. J. Predator inspection, shoaling and foraging under predation hazard in the Trinidadian guppy, Poecilia reticulata. *Environ Biol Fishes* **34**, 265–276 (1992).
24. Veilleux, C. C. & Kirk, E. C. Visual Acuity in Mammals: Effects of Eye Size and Ecology. *Brain Behav Evol* **83**, 43–53 (2014).
25. Caves, E. M., Sutton, T. T. & Johnsen, S. Visual acuity in ray-finned fishes correlates with eye size and habitat. *Journal of Experimental Biology* **220**, 1586–1596 (2017).
26. Caves, E. M., Brandley, N. C. & Johnsen, S. Visual Acuity and the Evolution of Signals. *Trends in Ecology and Evolution* vol. 33 358–372 Preprint at https://doi.org/10.1016/j.tree.2018.03.001 (2018).
27. Neave, D. A. The development of visual acuity in larval plaice (Pleuronectes platessa L.) and turbot (Scophthalmusmaximus L.). *J Exp Mar Biol Ecol* **78**, 167–175 (1984).
28. Anstis, S., Hutahajan, P. & Cavanagh, P. Optomotor test for wavelength sensitivity in guppyfish (Poecilia reticulata). *Vision Res* **38**, 45–53 (1998).

29. Haug, M. F., Biehlmaier, O., Mueller, K. P. & Neuhauss, S. C. F. Visual acuity in larval zebrafish: Behavior and histology. *Front Zool* **7**, 1–7 (2010).
30. Corral-López, A., Garate-Olaizola, M., Buechel, S. D., Kolm, N. & Kotrschal, A. On the role of body size, brain size, and eye size in visual acuity. *Behav Ecol Sociobiol* **71**, 1–10 (2017).
31. Corral-López, A. *et al.* Female brain size affects the assessment of male attractiveness during mate choice. *Sci Adv* **3**, e1601990 (2017).
32. Cronin, T. W., Johnsen, S., Marshall, N. J. & Warrant, E. J. *Visual Ecology*. *Visual Ecology* (Princeton University Press, 2014).
33. Kotrschal, A. *et al.* Artificial Selection on Relative Brain Size in the Guppy Reveals Costs and Benefits of Evolving a Larger Brain. *Current Biology* **23**, 168–171 (2013).
34. Fong, S. *et al.* Rapid mosaic brain evolution under artificial selection for relative telencephalon size in the guppy (Poecilia reticulata). *Sci Adv* **7**, eabj4314 (2021).
35. Handegard, N. O. *et al.* The dynamics of coordinated group hunting and collective information transfer among schooling prey. *Current Biology* **22**, 1213–1217 (2012).
36. Ioannou, C. C., Guttal, V. & Couzin, I. D. Predatory fish select for coordinated collective motion in virtual prey. *Science (1979)* **337**, 1212–1215 (2012).
37. Kotrschal, A. *et al.* Brain size affects female but not male survival under predation threat. *Ecol Lett* **18**, 646–652 (2015).
38. van der Bijl, W., Thyselius, M., Kotrschal, A. & Kolm, N. Brain size affects the behavioural response to predators in female guppies (Poecilia reticulata). *Proceedings of the Royal Society B: Biological Sciences* **282**, 20151132 (2015).
39. Sumpter, D. J. T., Szorkovszky, A., Kotrschal, A., Kolm, N. & Herbert-Read, J. E. Using activity and sociability to characterize collective motion. *Philosophical Transactions of the Royal Society B: Biological Sciences* **373**, 20170015 (2018).
40. Magurran, A. E., Seghers, B. H., Carvalho, G. R. & Shaw, P. W. Behavioural consequences of an artificial introduction of guppies (Poecilia reticulata) in N. Trinidad: Evidence for the evolution of anti-predator behaviour in the wild. *Proceedings of the Royal Society B: Biological Sciences* **248**, 117–122 (1992).
41. Clément, R. J. G. *et al.* Collective decision making in guppies: A cross-population comparison study in the wild. *Behavioral Ecology* **28**, 919–924 (2017).
42. MacGregor, H., Herbert-Read, J. & Ioannu, C. Information can explain the dynamics of group order in animal collective behaviour. *Nat Commun* **11**, 1–8 (2020).
43. Northmore, D. P. M. The Optic Tectum . *Encyclopedia of fish physiology: From genome to environment* **1**, 131–142 (2011).
44. Jones, M. R., Grillner, S. & Robertson, B. Selective projection patterns from subtypes of retinal ganglion cells to tectum and pretectum: Distribution and relation to behavior. *Journal of Comparative Neurology* **517**, 257–275 (2009).
45. Kotrschal, A. *et al.* Evolution of brain region volumes during artificial selection for relative brain size. *Evolution (N Y)* **71**, 2942–2951 (2017).
46. Kowalko, J. E. *et al.* Loss of schooling behavior in cavefish through sight-dependent and sight-independent mechanisms. *Current Biology* **23**, 1874–1883 (2013).
47. Suzuki, D. G., Pérez-Fernández, J., Wibble, T., Kardamakis, A. A. & Grillner, S. The role of the optic tectum for visually evoked orienting and evasive movements. *Proc Natl Acad Sci U S A* **116**, 15272–15281 (2019).
48. Mueller, T. What is the Thalamus in Zebrafish? *Front Neurosci* **6**, 64 (2012).

49. Goldberg, J. H., Farries, M. A. & Fee, M. S. Basal ganglia output to the thalamus: Still a paradox. *Trends Neurosci* **36**, 695–705 (2013).
50. Achim, K., Salminen, M. & Partanen, J. Mechanisms regulating GABAergic neuron development. *Cellular and Molecular Life Sciences* **71**, 1395–1415 (2014).
51. Chou, M. Y. *et al.* Social conflict resolution regulated by two dorsal habenular subregions in zebrafish. *Science (1979)* **352**, 87–90 (2016).
52. Duboué, E. R., Hong, E., Eldred, K. C. & Halpern, M. E. Left Habenular Activity Attenuates Fear Responses in Larval Zebrafish. *Current Biology* **27**, 2154–2162 (2017).
53. Kutsukake, N. Complexity, dynamics and diversity of sociality in group-living mammals. *Ecological Research* **24**, 521–531 (2009).
54. Lecchini, D. *et al.* Variation in brain organization of coral reef fish larvae according to life history traits. *Brain Behav Evol* **83**, 17–30 (2014).
55. Morita, Y. & Finger, T. E. Topographic representation of the sensory and motor roots of the vagus nerve in the medulla of goldfish, Carassius auratus. *J Comp Neurol* **264**, 231–249 (1987).
56. Vega-Trejo, R. *et al.* Artificial selection for schooling behaviour and its effects on associative learning abilities. *Journal of Experimental Biology* **223**, 235093 (2020).
57. Medan, V. & Preuss. T. The Mauthner-cell circuit of fish as a model system for startle plasticity. *Journal of Physiology-Paris* **108**, 129–140 (2014).
58. Fischer, E. K., Schwartz, A. J., Hoke, K. L. & Soares, D. Social context modulates predator evasion strategy in guppies. *Ethology* **121**, 364–371 (2015).
59. Kozloski, J. & Crawford, J. D. Transformations of an auditory temporal code in the medulla of a sound- producing fish. *Journal of Neuroscience* **20**, 2400–2408 (2000).
60. Finger, T. E. Evolution of gustatory reflex systems in the brainstems of fishes. *Integr Zool* **4**, 53–63 (2009).
61. Chen, Y. C. *et al.* Expression change in angiopoietin-1 underlies change in relative brain size in fish. *Proceedings of the Royal Society B: Biological Sciences* **282**, 20150872 (2015).
62. Partridge, B. L. & Pitcher, T. J. The sensory basis of fish schools: Relative roles of lateral line and vision. *Journal of comparative physiology* **135**, 315–325 (1980).
63. Szorkovszky, A. *et al.* An efficient method for sorting and quantifying individual social traits based on group-level behaviour. *Methods Ecol Evol* **8**, 1735–1744 (2017).
64. Pérez-Escudero, A., Vicente-Page, J., Hinz, R. C., Arganda, S. & de Polavieja, G. G. idTracker: tracking individuals in a group by automatic identification of unmarked animals. *Nature Methods 2014 11:7* **11**, 743–748 (2014).
65. Kotrschal, A. *et al.* Brain size does not impact shoaling dynamics in unfamiliar groups of guppies (Poecilia reticulata). *Behavioural Processes* **147**, 13–20 (2018).
66. Bates, D., Sarkar, D., Bates, M. D. & Matrix, L. The lme4 Package. *R package version* **2**, 74 (2007).
67. Kuznetsova, A., Brockhoff, P. B. & Christensen, R. H. B. lmerTest Package: Tests in Linear Mixed Effects Models. *J Stat Softw* **82**, 1–26 (2017).
68. Lenth, R. Package 'lsmeans'. *Am Stat* **34**, 216–221 (2018).
69. Friard, O. & Gamba, M. BORIS: a free, versatile open-source event-logging software for video/audio coding and live observations. *Methods Ecol Evol* **7**, 1325–1330 (2016).
70. Brooks, M. E. *et al.* glmmTMB balances speed and flexibility among packages for zero-inflated generalized linear mixed modeling. *R J* **9**, 378–400 (2017).

71. Hartig, F. DHARMa: residual diagnostics for hierarchical (multi-level/mixed) regression models. *R package version 0.3* (2018).
72. Bürkner, P. C. Advanced Bayesian multilevel modeling with the R package brms. *R J* **10**, 395–411 (2018).
73. Bürkner, P. C. brms: An R package for Bayesian multilevel models using Stan. *J Stat Softw* **80**, 1–28 (2017).
74. Carpenter, B. *et al.* Stan: A probabilistic programming language. *J Stat Softw* **76**, (2017).
75. Smith, K. U. & Bojar, S. The nature of optokinetic reactions in mammals and their significance in the experimental analysis of the neural mechanisms of visual functions. *Psychol Bull* **35**, 193–219 (1938).
76. Schneider, C. A., Rasband, W. S. & Eliceiri, K. W. NIH Image to ImageJ: 25 years of image analysis. *Nature Methods 2012 9:7* **9**, 671–675 (2012).
77. Schielzeth, H. *et al.* Robustness of linear mixed-effects models to violations of distributional assumptions. *Methods Ecol Evol* **11**, 1141–1152 (2020).
78. Koller, M. Robustlmm: An R package for Robust estimation of linear Mixed-Effects models. *J Stat Softw* **75**, 1–24 (2016).

Figures

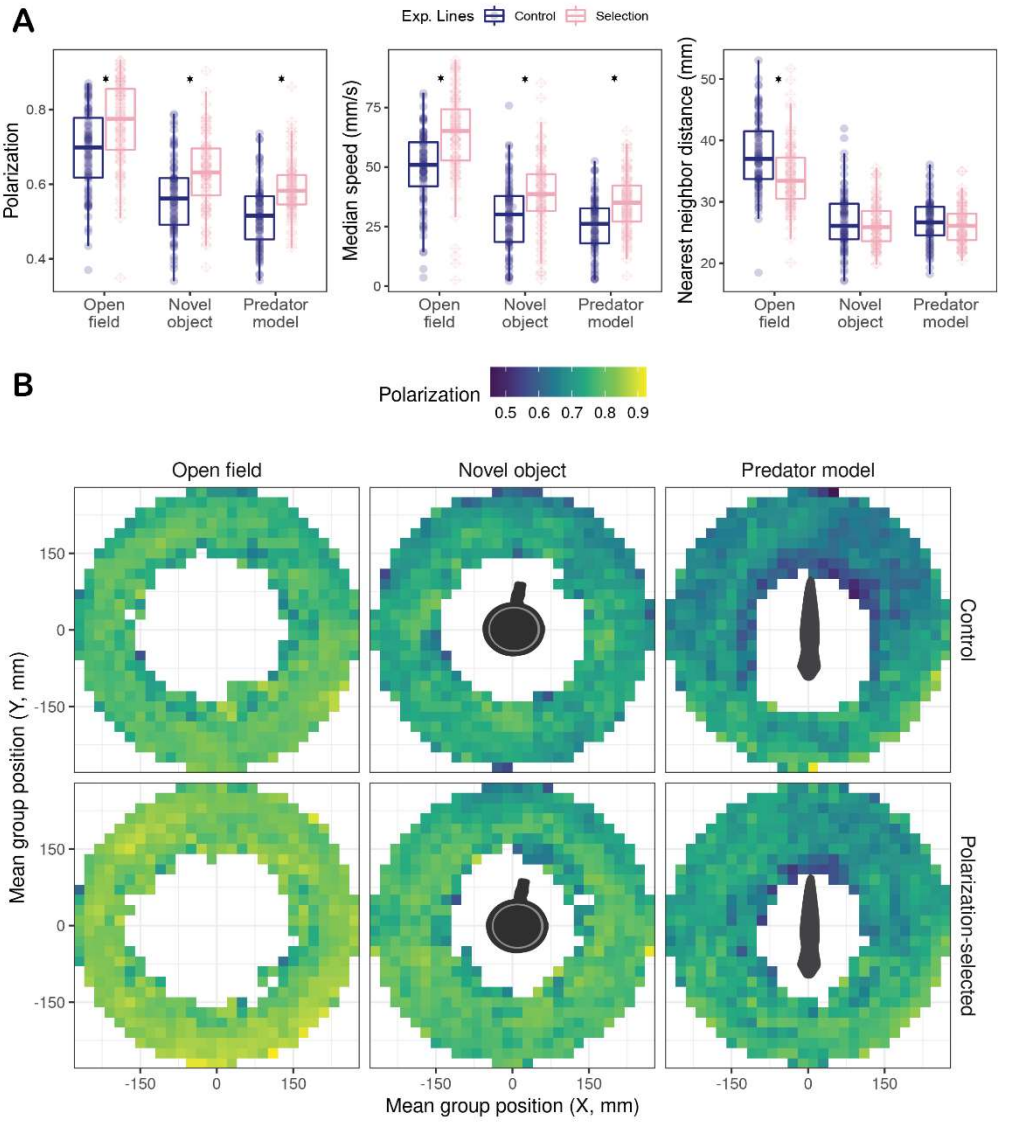

Fig 1. Collective motion patterns in female guppies artificially selected for higher schooling propensity. A) Boxplots of median polarization, speed and nearest neighbor distance for groups of eight individuals of polarization-selected (pink) and control (blue) female guppies assayed in an open field test (OFT), with a novel object and with a predator model. Horizontal lines indicate medians, boxes indicate the interquartile range, and whiskers indicate all points within 1.5 times the interquartile range. Asterisks indicate $p < 0.05$ (see methods; Supplementary Tables 1-2). **B)** Heatmaps of group polarization across different locations of the experimental arena when control (top) and polarization-selected (bottom) groups were exposed to open field, novel object and predator model assays. Grid cells with data for less than 8 groups were not depicted.

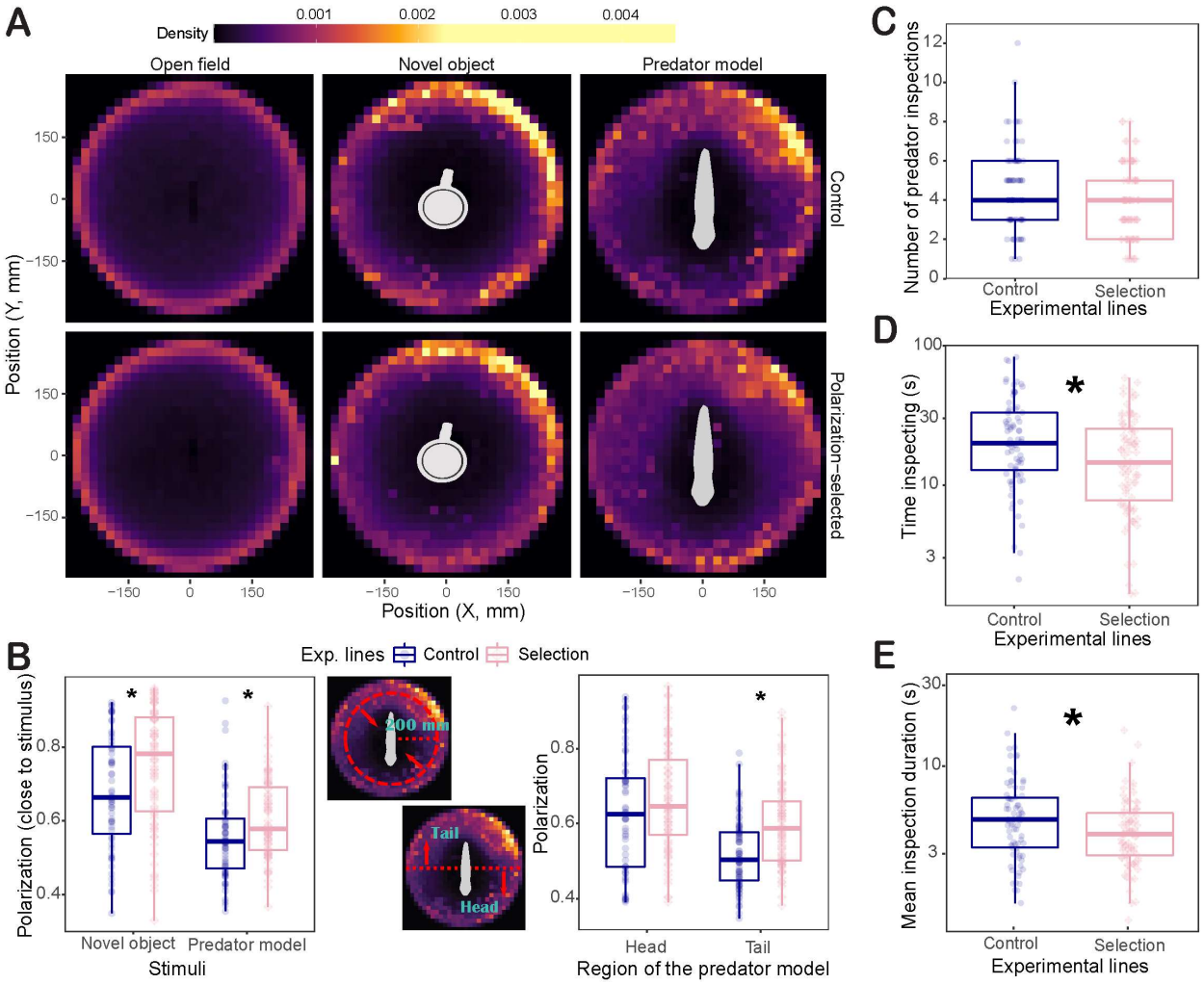

Fig 2. Social information processing in predator model assays. (A) Density maps based on positional data of control (top) and polarization-selected (bottom) groups exposed to open field, novel object and predator model assays. **(B)** Boxplots of median group polarization in locations closer than 200 mm of the stimulus presented (left) and in the head and tail area of a predator model (right) in control (blue) and polarization-selected (pink) guppy groups. Boxplots of number of predator inspections **(C)**, total time inspecting **(D),** and mean inspection duration **(E)** for individuals when swimming in a group of eight polarization-selected (pink) and control (blue) female guppies in the presence of a predator model. Horizontal lines indicate medians, boxes indicate the interquartile range, and whiskers indicate all points within 1.5 times the interquartile range. Asterisks indicate $p < 0.05$ (see methods, Supplementary Tables 5-7).

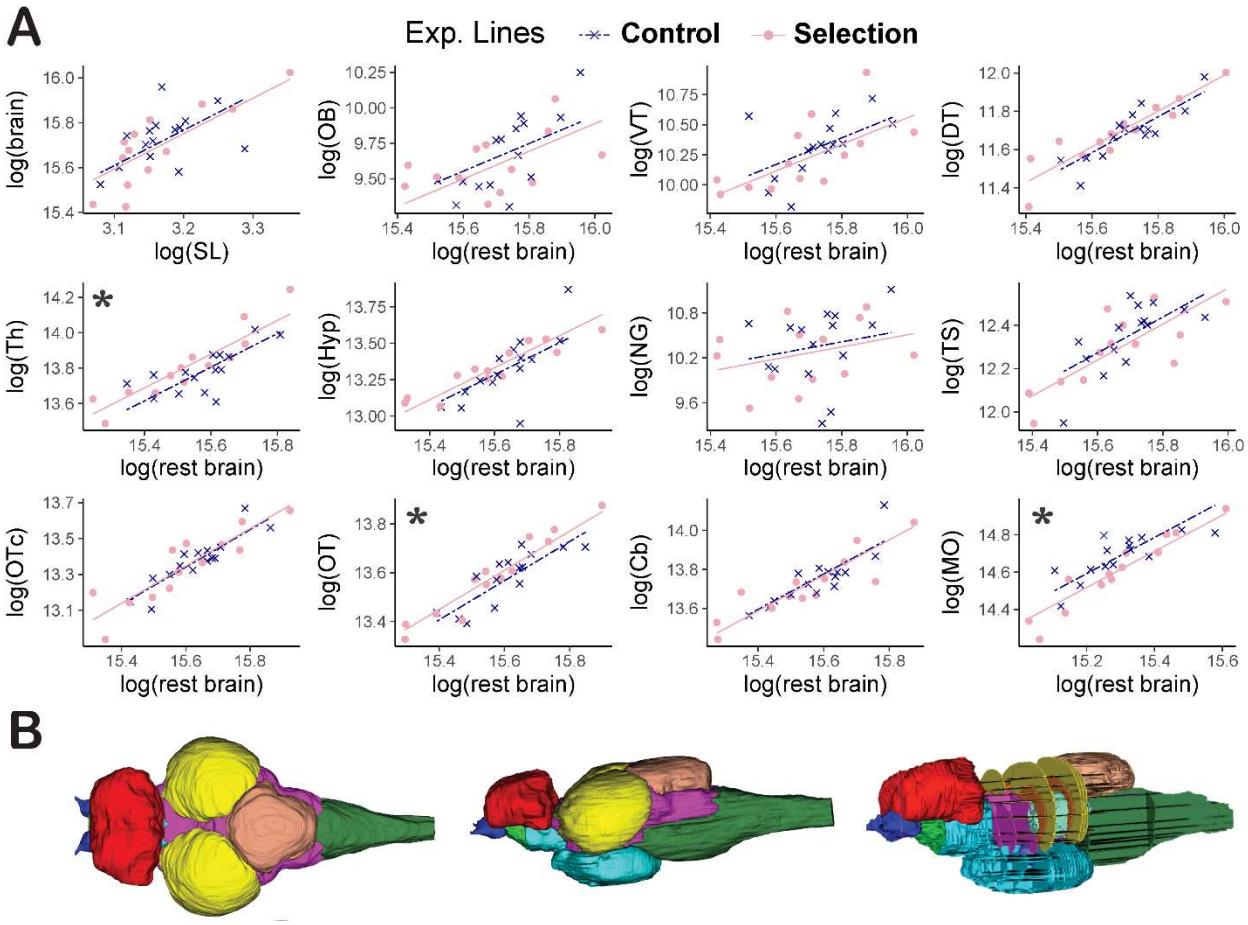

Fig 3. The effect of artificial selection for higher schooling propensity in neuroanatomical allometric relationships. (A) The top left panel shows the allometric relationship between whole brain size volume and standard length of the fish (SL). Remaining panels show the relationship between each separate brain region with the rest of the brain ordered rostrally to caudally. Asterisks indicate brain regions with non-overlapping confidence intervals between polarization-selected females (pink; n = 13) and control females (blue; n = 15) in two consistent statistical analyses (Supplementary Tables 3-4). **(B)** Reconstructed brain regions from micro CT - scanned guppy brains. A dorsal (left) and lateral (middle) view of a guppy brain with the major brain regions color coded: olfactory bulbs (OB; dark blue), dorsal telencephalon (DT; red), ventral telencephalon (VT; light green), optic tectum (OT; yellow), hypothalamus (Hyp; turquoise), thalamus (Th; purple), cerebellum (Cb; brown), medulla oblongata (MO; dark green); as some regions are not visible from the outside a partially segmented and slightly tilted image (right) reveals: torus semicircularis (TS; orange), nucleus glomerulus (NG; lilac-blue), optic tectum core (OTc; light turquoise).

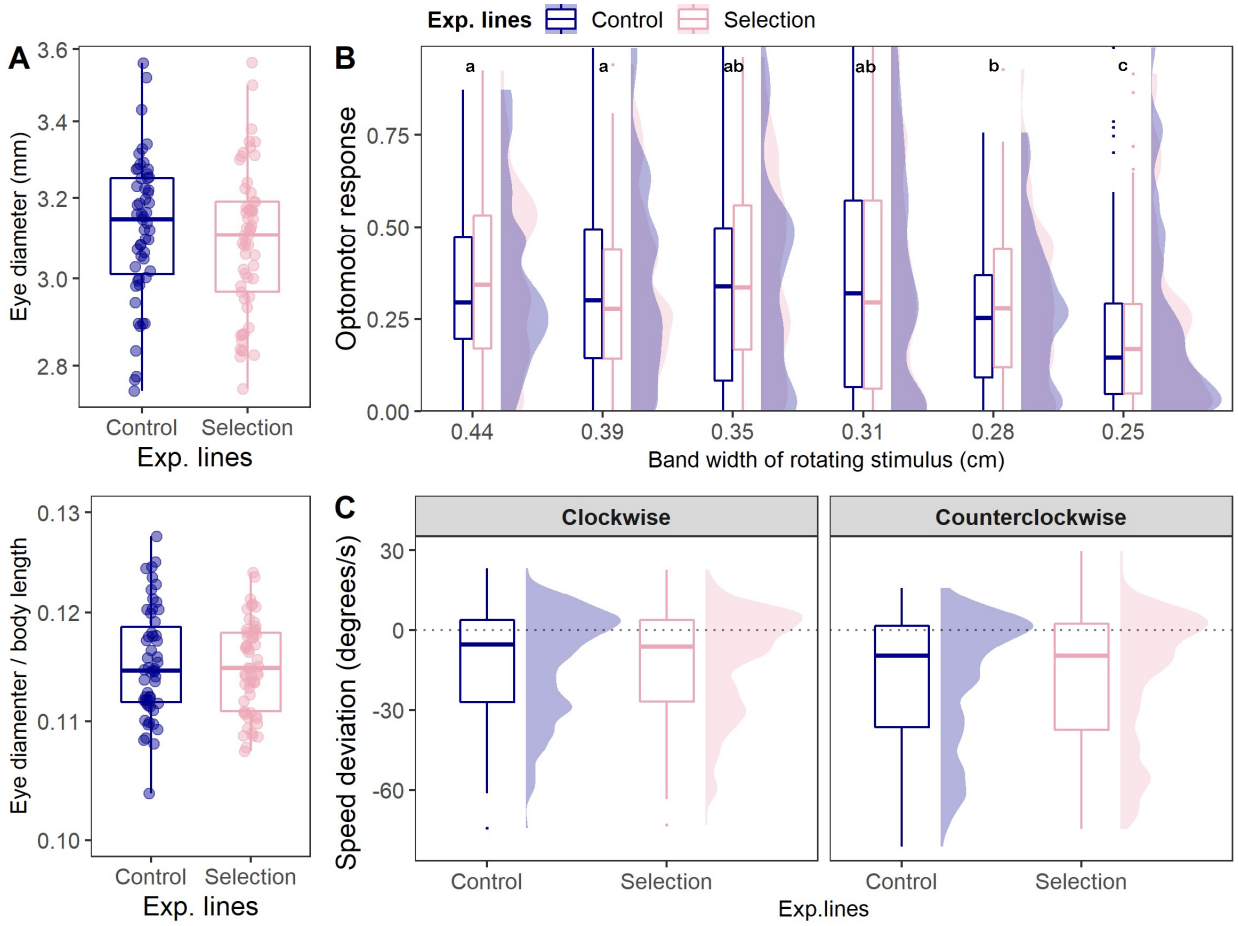

Fig 4. Eye morphology and visual capacities of female guppies artificially selected for higher schooling propensity. (A) Boxplots of eye morphological measurements. **(B)** Boxplots and density plots of the proportion of time following 6 different rotating stimuli with rotating and static gratings of different widths at the lower end of guppy visual acuity (thinner widths represent a higher degree of difficulty to be perceived). **(C)** Boxplots and density plots of the deviation of fish swimming speed in relation to the speed that a rotating stimulus presented. in polarization-selected. For all morphological measurements and vision assays we measured the same polarization-selected (pink; n = 57-59) and control females (blue; n = 55-57). In all boxplots, horizontal lines indicate medians, boxes indicate the interquartile range, and whiskers indicate all points within 1.5 times the interquartile range. Optomotor response average values not sharing any letter are significantly different ($p < 0.05$) in post-hoc contrasts (see Supplementary Table 9b). No significant differences were observed for any comparison between control and polarization-selected fish (see Supplementary Tables 8-10).

Supplementary Figures for:

Evolution of schooling propensity in the guppy drives changes in anti-predator behavior that are linked to neuroanatomy

Alberto Corral-Lopez*, Alexander Kotrschal, Alexander Szorkovszky, Maddi Garate-Olaizola, James Herbert-Read, Wouter van der Bijl, Maksym Romenskyy, Hong-Li Zeng, Severine Denise Buechel, Ada Fontrodona Eslava, Kristian Pelckmans, Judith E. Mank, Niclas Kolm

*corresponding author: corral@zoology.ubc.ca

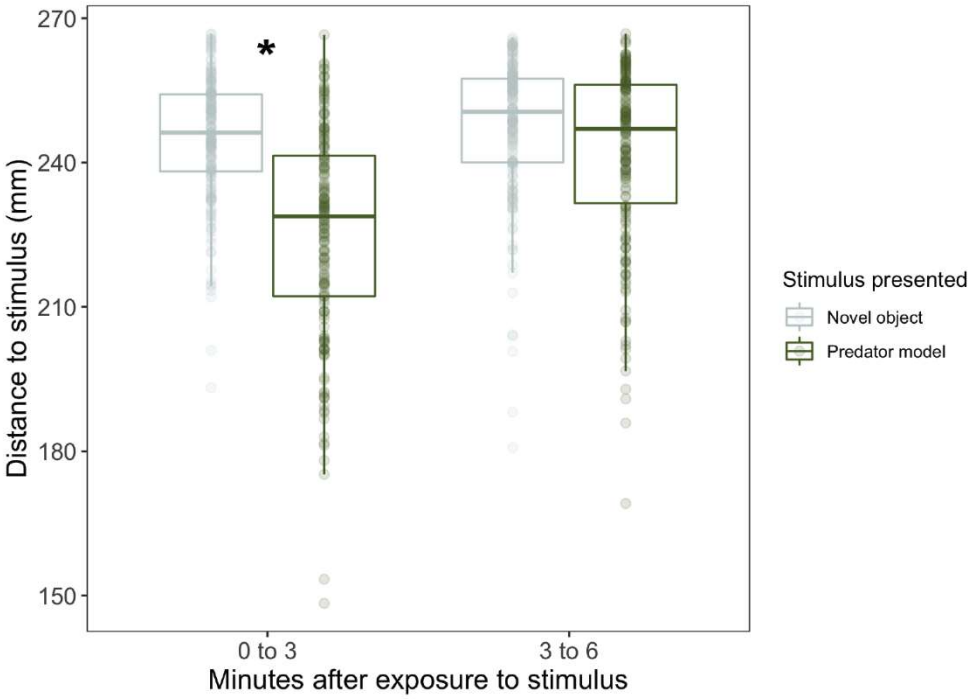

Fig S1. Proximity to stimuli in female guppies artificially selected for higher schooling propensity. Boxplots of median distance to the stimulus combining data for groups of polarization-selected and control female guppies (n = 164) in predator model and novel object assays. Horizontal lines indicate medians, boxes indicate the interquartile range, and whiskers indicate all points within 1.5 times the interquartile range. Asterisks indicate $p < 0.05$.

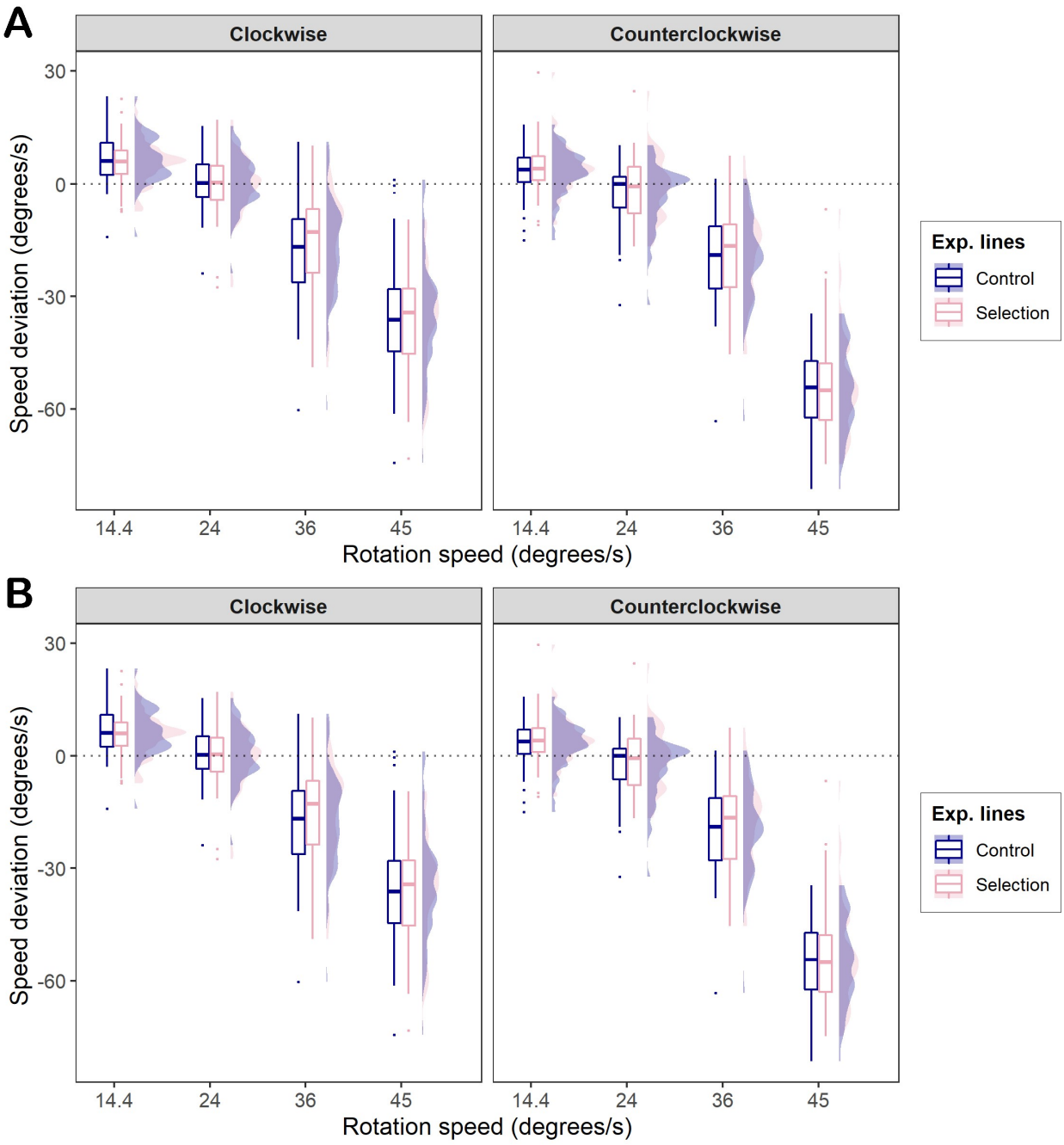

Fig S2. Temporal resolution of female guppies artificially selected for higher schooling propensity. Boxplots and density plots of the deviation of fish swimming speed **(A),** and the proportion of time that fish followed the direction of the stimulus **(B)** in relation to four different rotating stimuli presented at different speeds that rotated clockwise and anti-clockwise to polarization-selected (pink; n = 58) and control females (blue; n = 56). In the boxplots, horizontal lines indicate medians, boxes indicate the interquartile range, and whiskers indicate all points within 1.5 times the interquartile range. No significant differences were observed for any comparison between control and polarization-selected fish (see Tables S9-S10).

Supplementary Tables for:

Evolution of schooling propensity in the guppy drives changes in anti-predator behavior that are linked to neuroanatomy

Alberto Corral-Lopez*, Alexander Kotrschal, Alexander Szorkovszky, Maddi Garate-Olaizola, James Herbert-Read, Wouter van der Bijl, Maksym Romenskyy, Hong-Li Zeng, Severine Denise Buechel, Ada Fontrodona Eslava, Kristian Pelckmans, Judith E. Mank, Niclas Kolm

*corresponding author: corral@zoology.ubc.ca

Table S1. Statistical tests for overall comparisons in tests evaluating polarization-selected and control female guppies in their shoaling patterns when exposed to an open field test (OFT), a novel object (cup) and a predator model.

Polarization

Predictors	*Estimates*	*CI*	*t*	*p*	*df*
(Intercept)	0.80	0.68 – 0.91	14.54	**< 0.001**	17.59
Selection [P]	0.08	0.02 – 0.13	3.90	**0.017**	3.98
treatment [Cup]	-0.12	-0.15 – -0.10	-9.16	**< 0.001**	338.42
treatment [Predator]	-0.17	-0.20 – -0.14	-12.61	**< 0.001**	340.73
Body size	-0.00	-0.00 – -0.00	-2.35	**0.021**	88.01
Selection [P] * treatment [Cup]	-0.01	-0.05 – 0.03	-0.46	0.644	340.46
Selection [S] * treatment [Predator]	-0.00	-0.04 – 0.03	-0.18	0.860	341.08

Median speed

Predictors	*Estimates*	*CI*	*t*	*p*	*df*
(Intercept)	63.25	46.15 – 80.34	7.50	**< 0.001**	35.87
Selection [P]	13.63	8.09 – 19.16	5.96	**< 0.001**	6.29
treatment [Cup]	-20.14	-23.91 – -16.37	-10.51	**< 0.001**	337.87

treatment [Predator]	-24.34	-28.14 – -20.54	-12.60	**< 0.001**	339.82
Body size	-0.06	-0.12 – 0.01	-1.77	0.080	85.64
Selection [P] * treatment [Cup]	-4.55	-9.85 – 0.76	-1.69	0.093	339.52
Selection [S] * treatment [Predator]	-3.95	-9.27 – 1.36	-1.46	0.144	340.05

Nearest neighbor distance

Predictors	*Estimates*	*CI*	*t*	*p*	*df*
(Intercept)	39.17	33.89 – 44.45	14.96	**< 0.001**	43.22
Selection [P]	-3.43	-5.34 – -1.53	-4.55	**< 0.001**	5.31
treatment [Cup]	-10.77	-11.94 – -9.60	-18.13	**< 0.001**	337.80
treatment [Predator]	-10.88	-12.06 – -9.70	-18.17	**< 0.001**	339.69
Body size	-0.01	-0.03 – 0.01	-0.63	0.530	105.88
Selection [P] * treatment [Cup]	2.88	1.24 – 4.53	3.45	**< 0.001**	339.38
Selection [S] * treatment [Predator]	2.82	1.17 – 4.47	3.37	**< 0.001**	339.88

Table S2. Independent contrasts for comparisons between polarization-selected and control female guppies in their shoaling patterns when exposed to an open field test (OFT), a novel object (cup) and a predator model

Polarization

contrast	*treatment*	*estimate*	*SE*	*df*	*lower.CL*	*upper.CL*	*t.ratio*	*p.value*
C - P	OFT	-0.077	0.020	3.980	-0.133	-0.022	-3.898	**0.018**
C - P	Cup	-0.069	0.020	4.078	-0.124	-0.014	-3.435	**0.026**
C - P	Predator	-0.074	0.020	4.106	-0.129	-0.019	-3.698	**0.020**

Median speed

contrast	*treatment*	*estimate*	*SE*	*df*	*lower.CL*	*upper.CL*	*t.ratio*	*p.value*
C - P	OFT	-13.627	2.288	6.292	-19.164	-8.091	-5.956	**0.001**
C - P	Cup	-9.079	2.311	6.560	-14.619	-3.538	-3.928	**0.006**
C - P	Predator	-9.673	2.321	6.618	-15.226	-4.121	-4.168	**0.005**

Nearest neighbor distance

contrast	*treatment*	*estimate*	*SE*	*df*	*lower.CL*	*upper.CL*	*t.ratio*	*p.value*
C - P	OFT	3.434	0.754	5.309	1.530	5.339	4.555	**0.005**
C - P	Cup	0.552	0.761	5.510	-1.350	2.455	0.726	0.498
C - P	Predator	0.613	0.764	5.560	-1.292	2.517	0.802	0.455

Table S3. Statistical tests for comparisons in tests evaluating polarization-selected and control female guppies in their anti-predator behavior when exposed to a predator model

Number of inspections

Predictors	*Incidence Rate Ratios*	*CI*	*t*	*p*
(Intercept)	4.47	3.64 – 5.50	14.19	**< 0.001**
Selection [P]	0.87	0.75 – 1.01	-1.85	0.0645

Total time inspecting

Predictors	*Incidence Rate Ratios*	*CI*	*t*	*p*
(Intercept)	24.04	18.02 – 32.07	21.64	**< 0.001**
Selection [P]	0.79	0.66 – 0.95	-2.52	**0.011**

Mean inspection duration

Predictors	*Incidence Rate Ratios*	*CI*	*t*	*p*
(Intercept)	5.62	4.84 – 6.53	22.63	**< 0.001**
Selection [P]	0.82	0.69 – 0.96	-2.49	**0.013**

Table S4a. Statistical tests for overall comparisons of group polarization in polarization-selected and control female guppies when the average position of the group was shorter than 200 mm to the stimulus presented in the arena in tests that exposed these fish to a predator model and a novel object (cup).

Polarization (closer than 200 mm from the predator model)					
Predictors	*Estimates*	*CI*	*t*	*p*	*df*
(Intercept)	0.68	0.60 – 0.75	25.78	**< 0.001**	3.87
Selection [P]	0.07	0.02 – 0.12	2.96	**0.003**	273.80
treatment [Predator model]	-0.12	-0.16 – -0.08	-5.34	**< 0.001**	146.76
Replicate [Rep2]	0.00	-0.04 – 0.04	0.05	0.958	143.72
replicate [Rep3]	0.01	-0.03 – 0.05	0.32	0.749	142.38
Selection [P] * treatment [Predator model]	-0.03	-0.08 – 0.03	-0.83	0.405	143.99

Table S4b. Statistical tests for independent contrasts of group polarization in polarization-selected and control female guppies when swimming at a distance closer than 200 mm to the stimulus presented in the arena in tests that exposed these fish to a predator model and a novel object (cup).

contrast	*treatment*	*estimate*	*SE*	*df*	*lower.CL*	*upper.CL*	*t.ratio*	*p.value*
C - P	Cup	-0.070	0.024	273.79	-0.116	-0.023	-2.956	**0.003**
C - P	Predator	-0.044	0.022	272.27	-0.088	-0.000	-1.984	**0.048**

Table S5a. Statistical tests for overall comparisons of group polarization in polarization-selected and control female guppies when the average position of the group was located closer to the tail area or closer to the head area of the predator model

Polarization					
Predictors	*Estimates*	*CI*	*Statistic*	*p*	*df*
(Intercept)	0.62	0.54 – 0.71	22.54	**< 0.001**	3.15
Selection [P]	0.04	-0.03 – 0.10	1.53	0.191	4.58
location [tail]	-0.11	-0.14 – -0.07	-5.47	**< 0.001**	156.96
line [Social] * location [tail]	0.04	-0.01 – 0.09	1.64	0.103	150.99

Table S5b. Statistical tests for independent contrasts of group polarization in polarization-selected and control female guppies when the average position of the group was located closer to the tail area or closer to the head area of the predator model

contrast	*location*	*estimate*	*SE*	*df*	*lower.CL*	*upper.CL*	*t.ratio*	*p.value*
C - P	Head	-0.037	0.024	4.58	-0.102	0.027	-1.534	0.191
C - P	Tail	-0.080	0.023	3.63	-0.146	-0.013	-3.483	**0.030**

Table S6. Results from independent Linear Mixed Models evaluating differences in relative brain and relative brain region size between polarization-selected and control female guppies.

Region	Coefficent	Estimate	SE	df	t	P-value
Whole brain	Intercept	10.706	0.929	22.992	11.520	**< 0.001**
	Sel. Line (Polarization)	-0.015	0.037	23.296	-0.415	0.682
	Log (SL)	1.581	0.292	22.899	5.401	**< 0.001**
Olfactory bulbs	Intercept	-5.639	4.048	24.311	-1.393	0.176
	Sel. Line (Polarization)	-0.054	0.071	23.443	-0.759	0.455
	Log (rest of brain)	0.973	0.257	24.319	3.782	**< 0.001**
Ventral telencephalon	Intercept	-7.112	4.022	23.970	-1.768	0.0897
	Sel. Line (Polarization)	-0.054	0.070	23.366	-0.762	0.453
	Log (rest of brain)	1.107	0.255	23.968	4.329	**< 0.001**
Dorsal telencephalon	Intercept	-3.002	1.502	25.000	-1.998	0.0567
	Sel. Line (Polarization)	0.029	0.027	25.000	1.096	0.2837
	Log (rest of brain)	0.935	0.095	25.000	9.780	**< 0.001**
Thalamus	Intercept	-1.019	1.805	25.000	-0.565	0.577
	Sel. Line (Polarization)	0.073	0.033	25.000	2.187	**0.038**
	Log (rest of brain)	0.950	0.115	25.000	8.197	**< 0.001**
Hypothalamus	Intercept	-3.858	2.745	25.000	-1.405	0.172
	Sel. Line (Polarization)	0.048	0.049	25.000	0.974	0.339
	Log (rest of brain)	1.098	0.175	25.000	6.259	**< 0.001**
Nucleus glomerulus	Intercept	-2.352	9.716	25.000	-0.242	0.811
	Sel. Line (Polarization)	-0.067	0.176	25.000	-0.381	0.706
	Log (rest of brain)	0.807	0.617	25.000	1.308	0.203
Torus semicircularis	Intercept	-0.665	2.368	24.977	-0.281	0.781
	Sel. Line (Polarization)	-0.0325	0.042	24.106	-0.758	0.456
	Log (rest of brain)	0.829	0.150	24.982	5.496	**< 0.001**
Optic tectum cup	Intercept	1.073	0.966	23.494	1.111	0.2780
	Sel. Line (Polarization)	0.042	0.017	23.095	2.409	**0.024**
	Log (rest of brain)	0.800	0.061	23.474	12.933	**< 0.**001
Optic tectum core	Intercept	-2.883	1.658	25.000	-1.739	0.0944
	Sel. Line (Polarization)	0.006	0.030	25.000	0.211	0.8347
	Log (rest of brain)	1.040	0.106	25.000	9.805	**< 0.001**
Cerebellum	Intercept	-0.403	1.458	24.350	-0.277	0.784
	Sel. Line (Polarization)	-0.007	0.026	23.221	-0.275	0.786
	Log (rest of brain)	0.908	0.093	24.358	9.703	**< 0.001**
Medulla oblongata	Intercept	-0.145	1.519	24.920	-0.096	0.9246
	Sel. Line (Polarization)	-0.074	0.028	23.916	-2.656	**0.013**
	Log (rest of brain)	0.969	0.099	24.935	9.761	**< 0.001**

Table S7a Results from a Bayesian multilevel model evaluating differences in relative brain region size between polarization-selected and control female guppies. Stars indicate estimates that do not include zero in the confidence interval range based on the posterior samples drawn from the model.

Covariate	*Estimate*	*Est.Error*	*l.95..CI*	*u.95..CI*	
Medulla_Intercept	0.19	0.32	-0.37	0.77	
Cerebellum_Intercept	0.05	0.50	-1.08	1.04	
Nucleus glomerulus_Intercept	0.09	0.48	-0.84	1.04	
Torus semicircularis_Intercept	0.14	0.44	-0.69	1.03	
Thalamus_Intercept	-0.25	0.34	-0.97	0.31	
Optic tectum cups_Intercept	-0.19	0.51	-1.26	0.89	
Hypothalamus_Intercept	-0.06	0.39	-0.84	0.73	
Olfactory bulbs_Intercept	0.13	0.54	-0.94	1.26	
Ventral telencephalon_Intercept	0.05	0.63	-1.23	1.43	
Dorsal telencephalon_Intercept	-0.09	0.32	-0.72	0.56	
Optic tectum core_Intercept	-0.02	0.28	-0.56	0.54	
Medulla oblongata_Selection	-0.42	0.18	**-0.79**	**-0.06**	*
Medulla oblongata_Rest of the brain	0.91	0.09	**0.74**	**1.09**	*
Cerebellum_Selection	-0.07	0.21	-0.48	0.35	
Cerebellum_Rest of the brain	0.96	0.11	**0.75**	**1.18**	*
Nucleus glomerolus_Selection	-0.21	0.40	-0.98	0.58	
Nucleus glomerulus_Rest of the brain	0.34	0.20	-0.06	0.75	
Torus semicircularis_Selection	-0.24	0.32	-0.87	0.38	
Torus semicircularis_Rest of the brain	0.72	0.16	**0.40**	**1.04**	*
Thalamus_Selection	0.49	0.23	**0.04**	**0.94**	*
Thalamus_Rest of the brain	0.92	0.11	**0.70**	**1.16**	*
Optic tectum cups_Selection	0.32	0.16	**0.00**	**0.63**	*
Optic tectum cups_Rest of the brain	0.88	0.08	**0.72**	**1.06**	*
Hypothalamus_Selection	0.12	0.26	-0.39	0.64	

Hypothalamus_Rest of the brain	0.87	0.13	**0.61**	**1.14**	*
Olfactory bulbs _Selection	-0.27	0.33	-0.93	0.38	
Olfactory bulbs_Rest of the brain	0.62	0.17	**0.29**	**0.95**	*
Ventral telencephalon_Selection	-0.17	0.31	-0.76	0.43	
Ventral telencephalon_Rest of the brain	0.58	0.16	**0.27**	**0.89**	*
Dorsal telencephalon_Selection	0.18	0.21	-0.25	0.60	
Dorsal telencephalon_Rest of the brain	0.91	0.11	**0.69**	**1.13**	*
Optic tectum core_Selection	0.05	0.20	-0.34	0.44	
Optic tectum core_Rest of the brain	0.93	0.10	**0.73**	**1.13**	*

Table S7b. Residual correlations of thalamus, optic tectum cups and medulla oblongata relative volume to other brain regions estimated from a Bayesian multilevel model evaluating differences in relative brain region size between polarization-selected and control female guppies. Stars indicate estimates that do not include zero in the confidence interval range based on the posterior samples drawn from the model.

Medulla oblongata

Brain region	*Estimate*	*Est.Error*	*l.95..CI*	*u.95..CI*	
Cerebellum	-0.32	0.15	**-0.59**	**-0.02**	*
Nucleus glomerulus	-0.26	0.15	-0.53	0.05	
Torus semicircularis	0.07	0.16	-0.25	0.37	
Thalamus	-0.40	0.14	**-0.65**	**-0.12**	*
Optic tectum cups	-0.04	0.17	-0.36	0.29	
Hypothalamus	-0.50	0.12	**-0.72**	**-0.23**	*
Olfactory bulbs	-0.24	0.16	-0.52	0.09	
Ventral telencephalon	-0.15	0.16	-0.44	0.17	
Dorsal telencephalon	-0.12	0.17	-0.43	0.21	
Optic tectum core	-0.22	0.15	-0.51	0.09	

Optic tectum cups

Brain region	*Estimate*	*Est.Error*	*l.95..CI*	*u.95..CI*
Medulla oblongata	-0.04	0.16	-0.36	0.28
Cerebellum	-0.07	0.17	-0.41	0.26
Nucleus glomerulus	-0.07	0.17	-0.40	0.26
Torus semicircularis	0.05	0.17	-0.29	0.38
Thalamus	-0.18	0.16	-0.49	0.15
Hypothalamus	-0.15	0.16	-0.46	0.17

Olfactory bulbs	-0.11	0.17	-0.45	0.23	
Ventral telencephalon	0.02	0.17	-0.32	0.36	
Dorsal telencephalon	-0.01	0.17	-0.36	0.33	
Optic tectum core	-0.06	0.17	-0.39	0.27	

Thalamus

Brain region	***Estimate***	***Est.Error***	***l.95..CI***	***u.95..CI***	
Medulla oblongata	-0.40	0.14	**-0.65**	**-0.12**	*
Cerebellum	-0.27	0.16	-0.55	0.05	
Nucleus glomerulus	0.05	0.16	-0.26	0.36	
Torus semicircularis	-0.27	0.16	-0.56	0.06	
Optic tectum cups	-0.18	0.17	-0.49	0.15	
Hypothalamus	-0.15	0.16	-0.44	0.18	
Olfactory bulbs	-0.09	0.16	-0.41	0.24	
Ventral telencephalon	0.27	0.16	-0.05	0.56	
Dorsal telencephalon	-0.05	0.17	-0.37	0.28	
Optic tectum core	0.10	0.16	-0.22	0.41	

Table S8. Statistical tests for comparisons in eye morphology between polarization-selected and control female guppies.

Eye diameter					
Predictors	*Estimates*	*CI*	*Statistic*	*p*	*df*
(Intercept)	3.12	2.95 – 3.29	78.98	**< 0.001**	2.00
Selection [P]	-0.03	-0.24 – 0.19	-0.52	0.658	2.00
Eye diameter / body length					
Predictors	*Estimates*	*CI*	*Statistic*	*p*	*df*
(Intercept)	0.12	0.11 – 0.12	69.97	**< 0.001**	2.00
Selection [P]	-0.00	-0.01 – 0.01	-0.13	0.906	2.00

Table S9a. Statistical tests for comparisons in visual acuity between polarization-selected and control female guppies.

Optomotor response					
Predictors	*Estimates*	*CI*	*Statistic*	*p*	*df*
(Intercept)	0.10	0.03 – 0.17	3.16	**0.008**	12.06
Selection [P]	0.00	-0.08 – 0.09	0.11	0.913	12.88
Band width stimulus [0.28]	0.07	0.00 – 0.14	2.09	**0.036**	570.82
Band width stimulus [0.31]	0.15	0.08 – 0.21	4.20	**< 0.001**	569.22
Band width stimulus [0.35]	0.12	0.05 – 0.19	3.51	**< 0.001**	569.28
Band width stimulus [0.39]	0.18	0.12 – 0.25	5.26	**< 0.001**	574.04
Band width stimulus [0.44]	0.17	0.10 – 0.23	4.75	**< 0.001**	572.07
Optomotor response in static	0.56	0.49 – 0.63	14.92	**< 0.001**	531.69
Selection [P]* Band width stimulus [0.28]	0.01	-0.08 – 0.11	0.26	0.793	569.30
Selection [P]* Band width stimulus [0.31]	0.01	-0.09 – 0.10	0.11	0.915	569.21
Selection [P]* Band width stimulus [0.35]	0.03	-0.06 – 0.13	0.63	0.526	569.18
Selection [P]* Band width stimulus [0.39]	-0.03	-0.13 – 0.06	-0.64	0.520	569.16
Selection [P]* Band width stimulus [0.44]	0.01	-0.09 – 0.10	0.17	0.863	569.22

Table S9b. Independent contrasts for optomotor response observed in fish at rotating stimulus of several band widths

contrast	*estimate*	*SE*	*df*	*lower.CL*	*upper.CL*	*t.ratio*	*p.value*
bw25 - bw28	-0.079	0.024	571.167	-0.149	-0.009	-3.236	**0.016**

bw25 - bw31	-0.148	0.024	569.618	-0.218	-0.079	-6.094	< **0.001**
bw25 - bw35	-0.137	0.024	569.230	-0.207	-0.068	-5.637	< **0.001**
bw25 - bw39	-0.168	0.025	577.744	-0.238	-0.097	-6.818	< **0.001**
bw25 - bw44	-0.169	0.024	573.616	-0.239	-0.099	-6.918	< **0.001**
bw28 - bw31	-0.069	0.024	569.653	-0.139	0.000	-2.852	0.051
bw28 - bw35	-0.058	0.024	570.338	-0.128	0.011	-2.390	0.161
bw28 - bw39	-0.089	0.024	571.492	-0.159	-0.019	-3.639	**0.004**
bw28 - bw44	-0.090	0.024	569.612	-0.160	-0.021	-3.712	**0.003**
bw31 - bw35	0.011	0.024	569.262	-0.058	0.081	0.460	0.997
bw31 - bw39	-0.019	0.025	574.211	-0.089	0.051	-0.791	0.969
bw31 - bw44	-0.021	0.024	571.155	-0.091	0.049	-0.858	0.956
bw35 - bw39	-0.031	0.025	575.985	-0.101	0.040	-1.245	0.814
bw35 - bw44	-0.032	0.024	572.350	-0.102	0.038	-1.315	0.777
bw39 - bw44	-0.002	0.024	569.833	-0.071	0.068	-0.064	1.000

Table S9c. Independent contrasts for optomotor response observed in polarization-selected and control female guppies at rotating stimulus of several band widths.

contrast	*stimulus*	*estimate*	*SE*	*df*	*lower.CL*	*upper.CL*	*t.ratio*	*p.value*
C - P	bw25	-0.004	0.038	601.455	-0.078	0.070	-0.112	0.911
C - P	bw28	-0.017	0.038	601.441	-0.091	0.057	-0.456	0.649
C - P	bw31	-0.009	0.038	601.422	-0.083	0.064	-0.247	0.805
C - P	bw35	-0.035	0.038	601.457	-0.109	0.039	-0.938	0.349
C - P	bw39	0.027	0.038	601.458	-0.047	0.101	0.722	0.471
C - P	bw44	-0.013	0.038	601.452	-0.086	0.061	-0.340	0.734

Table S10a. Statistical tests for comparisons in visual temporal resolution between polarization-selected and control female guppies.

Speed deviation from stimulus rotation

Predictors	*Estimates*	*CI*	*Statistic*	*p*	*df*
(Intercept)	8.38	3.23 – 13.53	5.31	**0.014**	2.87
Selection [P]	-0.46	-8.74 – 7.83	-0.19	0.863	2.64
Speed [24]	-5.93	-7.71 – -4.15	-6.54	**< 0.001**	4398.86
Speed [36]	-23.39	-25.17 – -21.61	-25.78	**< 0.001**	4398.86
Speed [45]	-49.74	-51.52 – -47.96	-54.79	**< 0.001**	4398.84
Rotation[Counterclockwise]	-7.11	-8.36 – -5.85	-11.08	**< 0.001**	4398.89
Selection [P] * Speed [24]	0.31	-2.17 – 2.79	0.25	0.805	4398.91
Selection [P] * Speed [36]	1.26	-1.22 – 3.74	0.99	0.320	4398.91
Selection [P] * Speed [45]	-0.48	-2.96 – 1.99	-0.38	0.701	4398.84
Selection [P] * Rotation[Counterclockwise]	1.29	-0.47 – 3.04	1.44	0.150	4398.98

Proportion of time following the stimulus

Predictors	*Estimates*	*CI*	*Statistic*	*p*	*df*
(Intercept)	0.87	0.80 – 0.94	39.43	**< 0.001**	3.12
Selection [P]	0.00	-0.14 – 0.15	0.10	0.928	2.52
Speed [24]	0.03	0.00 – 0.06	2.03	**< 0.001**	4398.95
Speed [36]	0.03	-0.00 – 0.05	1.83	0.067	4398.95
Speed [45]	-0.04	-0.06 – -0.01	-2.55	**0.018**	4398.92
Rotation[Counterclockwise]	-0.07	-0.09 – -0.05	-7.33	**< 0.001**	4398.98
Selection [P] * Speed [24]	0.01	-0.02 – 0.04	0.74	0.457	4399.06
Selection [P] * Speed [36]	-0.00	-0.04 – 0.03	-0.20	0.843	4398.99
Selection [P] * Speed [45]	-0.00	-0.04 – 0.04	-0.15	0.884	4398.99

Selection [P] * Rotation[Counterclockwise]	-0.01	-0.05 – 0.03	-0.62	0.536	4398.92

Table S10b. Independent contrasts for speed deviation to stimulus rotation observed in polarization-selected and control females at multiple rotation speeds in clockwise and counterclockwise directions

Selection	*Speed*	*Rotation*	*emmean*	*SE*	*df*	*lower.CL*	*upper.CL*	*t.ratio*	*p.value*
C	14.4	Clockwise	8.379	1.577	2.874	3.233	13.526	5.313	**0.015**
P	14.4	Clockwise	7.922	1.938	2.485	0.966	14.879	4.089	**0.038**
C	24	Clockwise	2.447	1.577	2.872	-2.701	7.594	1.552	0.222
P	24	Clockwise	2.303	1.938	2.488	-4.650	9.256	1.188	0.336
C	36	Clockwise	-15.012	1.577	2.872	-20.160	-9.865	-9.520	**0.003**
P	36	Clockwise	-14.212	1.938	2.488	-21.164	-7.259	-7.332	**0.010**
C	45	Clockwise	-41.357	1.577	2.874	-46.503	-36.210	-26.223	**< 0.001**
P	45	Clockwise	-42.299	1.938	2.485	-49.255	-35.342	-21.830	**0.001**
C	14.4	Counterclockwise	1.272	1.577	2.873	-3.875	6.420	0.807	0.481
P	14.4	Counterclockwise	2.103	1.938	2.487	-4.850	9.057	1.085	0.372
C	24	Counterclockwise	-4.660	1.577	2.869	-9.809	0.489	-2.956	0.063
P	24	Counterclockwise	-3.517	1.939	2.491	-10.465	3.432	-1.814	0.186
C	36	Counterclockwise	-0.483	-22.119	1.577	2.869	-27.268	-14.030	**0.001**
P	36	Counterclockwise	-20.031	1.939	2.491	-26.979	-13.083	-10.331	**0.004**
C	45	Counterclockwise	-48.464	1.577	2.873	-53.611	-43.317	-30.731	**< 0.001**
P	45	Counterclockwise	-48.118	1.938	2.487	-55.071	-41.164	-24.827	**< 0.001**

Table S11. Statistical results using a robust linear mixed model approach for comparisons in the proportion of time following the correct direction of the stimulus in visual temporal assays between polarization-selected and control female guppies.

Proportion of time following the stimulus

Predictors	*Estimates*	*Std. Error*	*t-value*	*p*	*df*
(Intercept)	0.91	0.016	57.45	**< 0.001**	3.12
Selection [P]	-0.001	0.031	-0.04	0.971	2.52
Speed [24]	0.014	0.009	1.61	0.106	4398.95
Speed [36]	0.027	0.009	3.07	**0.001**	4398.95
Speed [45]	-0.010	0.009	-1.17	0**.240**	4398.92
Rotation[Counterclockwise]	-0.041	0.006	-6.51	**< 0.001**	4398.98
Selection [P] * Speed [24]	0.004	0.012	0.33	0.744	4399.06
Selection [P] * Speed [36]	0.004	0.012	0.33	0.741	4398.99
Selection [P] * Speed [45]	-0.009	0.012	-0.74	0.460	4398.99
Selection [P] * Rotation[Counterclockwise]	-0.001	0.009	-0.15	0.882	4398.92

Robustness weights for the residuals:
3546 weights are ~= 1. The remaining 974 ones are summarized as
 Min. 1st Qu. Median Mean 3rd Qu. Max.
0.199 0.328 0.518 0.557 0.773 0.999

Robustness weights for the random effects:
101 weights are ~= 1. The remaining 18 ones are summarized as
 Min. 1st Qu. Median Mean 3rd Qu. Max.
0.247 0.489 0.739 0.693 0.904 0.995

Rho functions used for fitting:
Residuals:
 eff: smoothed Huber (k = 1.345, s = 10), sig: smoothed Huber, Proposal II (k = 1.345, s = 10)
Random Effects, variance component 1 (trial):
 eff: smoothed Huber (k = 1.345, s = 10), vcp: smoothed Huber, Proposal II (k = 1.345, s = 10)
Random Effects, variance component 2 (rep):
 eff: smoothed Huber (k = 1.345, s = 10), vcp: smoothed Huber (k = 1.345, s = 10)

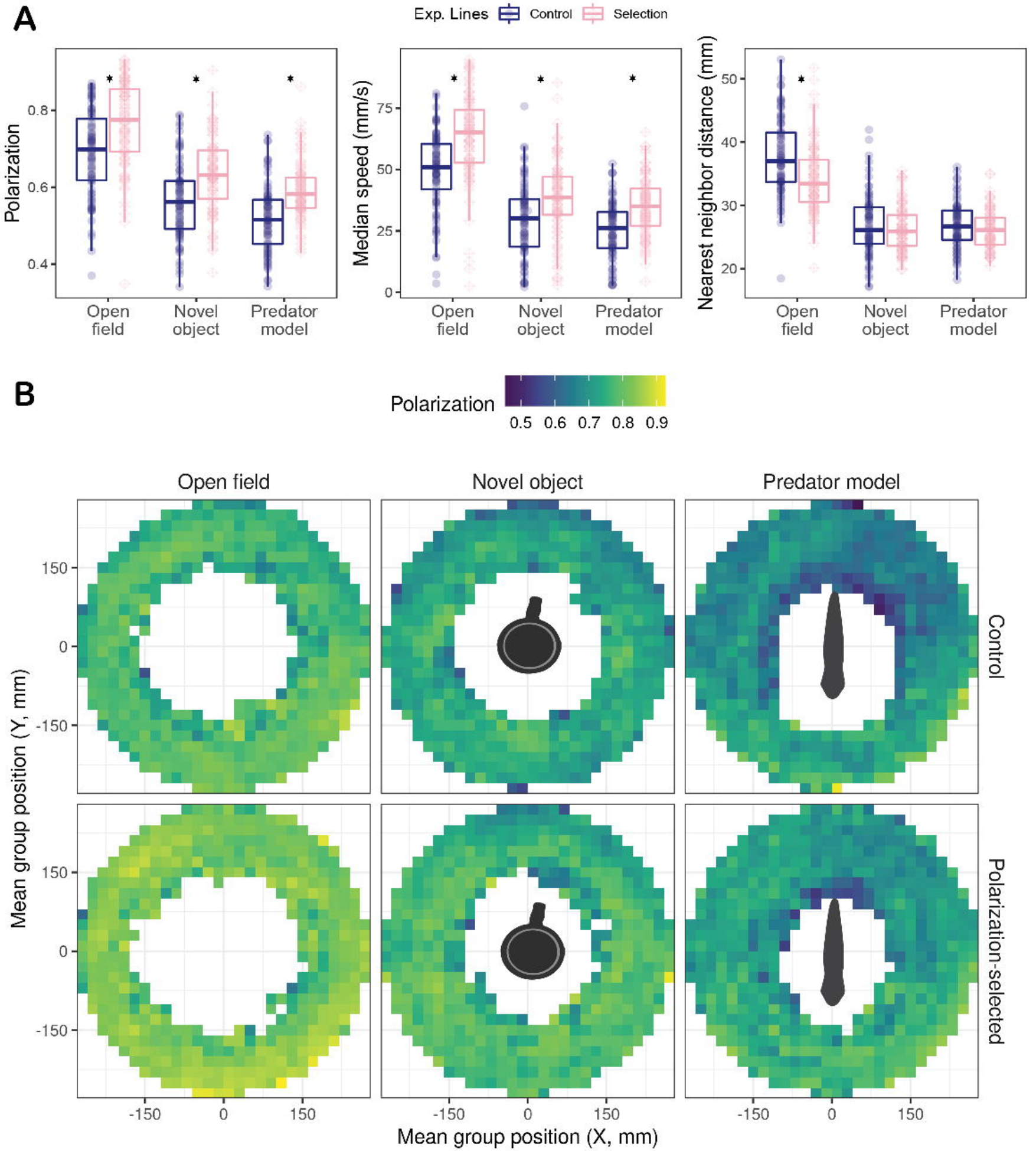
A
Exp. Lines
Control
Selection
Polarization
Median speed (mm/s)
Nearest neighbor distance (mm)
Open field
Novel object
Predator model
B
Polarization
0.5 0.6 0.7 0.8 0.9
Open field
Novel object
Predator model
Control
Polarization-selected
Mean group position (Y, mm)
Mean group position (X, mm)

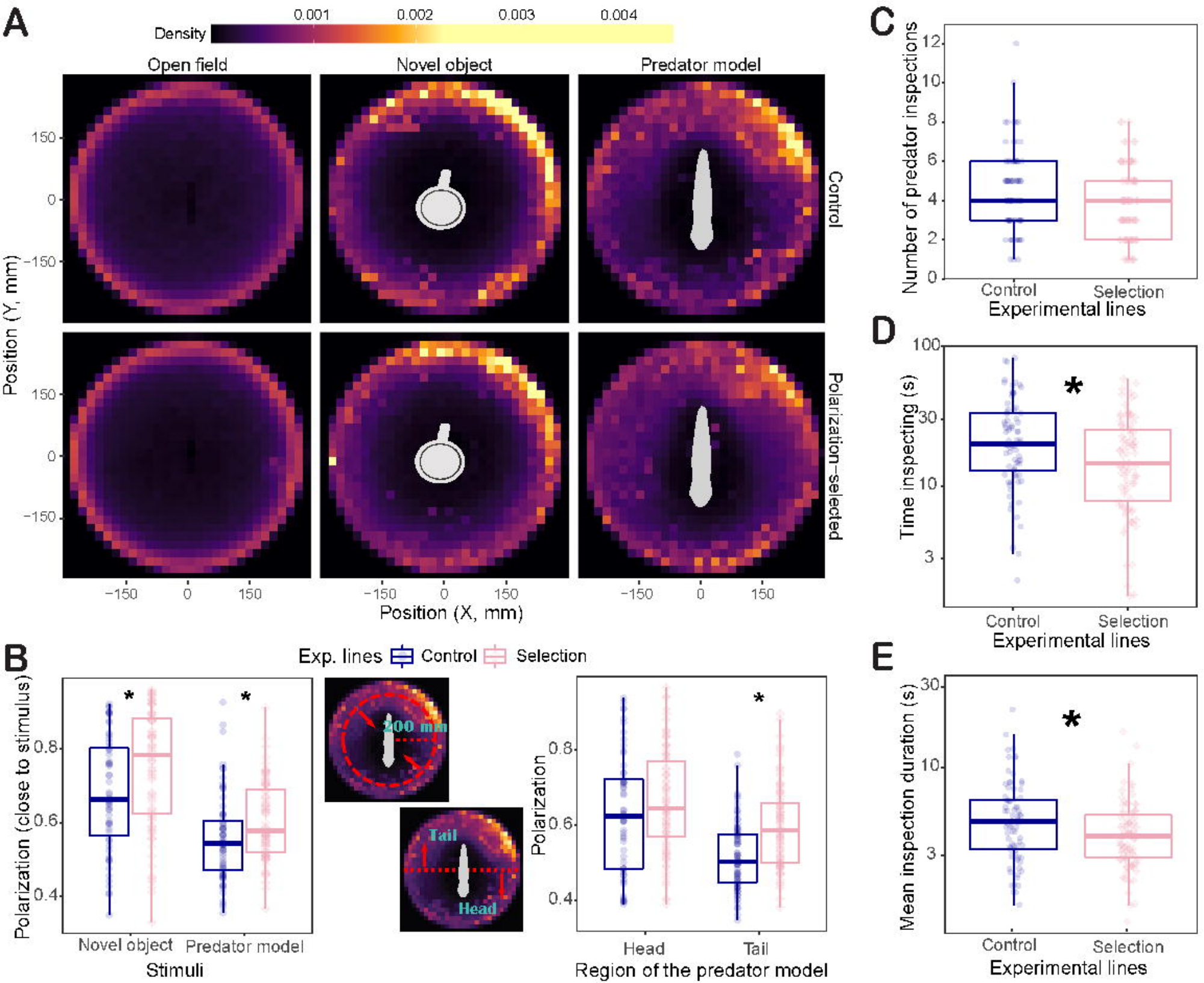
A
Density
0.001
0.002
0.003
0.004
Open field
Novel object
Predator model
Control
Polarization−selected
Position (Y, mm)
Position (X, mm)
150
0
−150
B
Exp. lines
Control
Selection
Polarization (close to stimulus)
Novel object
Predator model
Stimuli
200 mm
Tail
Head
Polarization
Region of the predator model
C
Number of predator inspections
Experimental lines
D
Time inspecting (s)
E
Mean inspection duration (s)

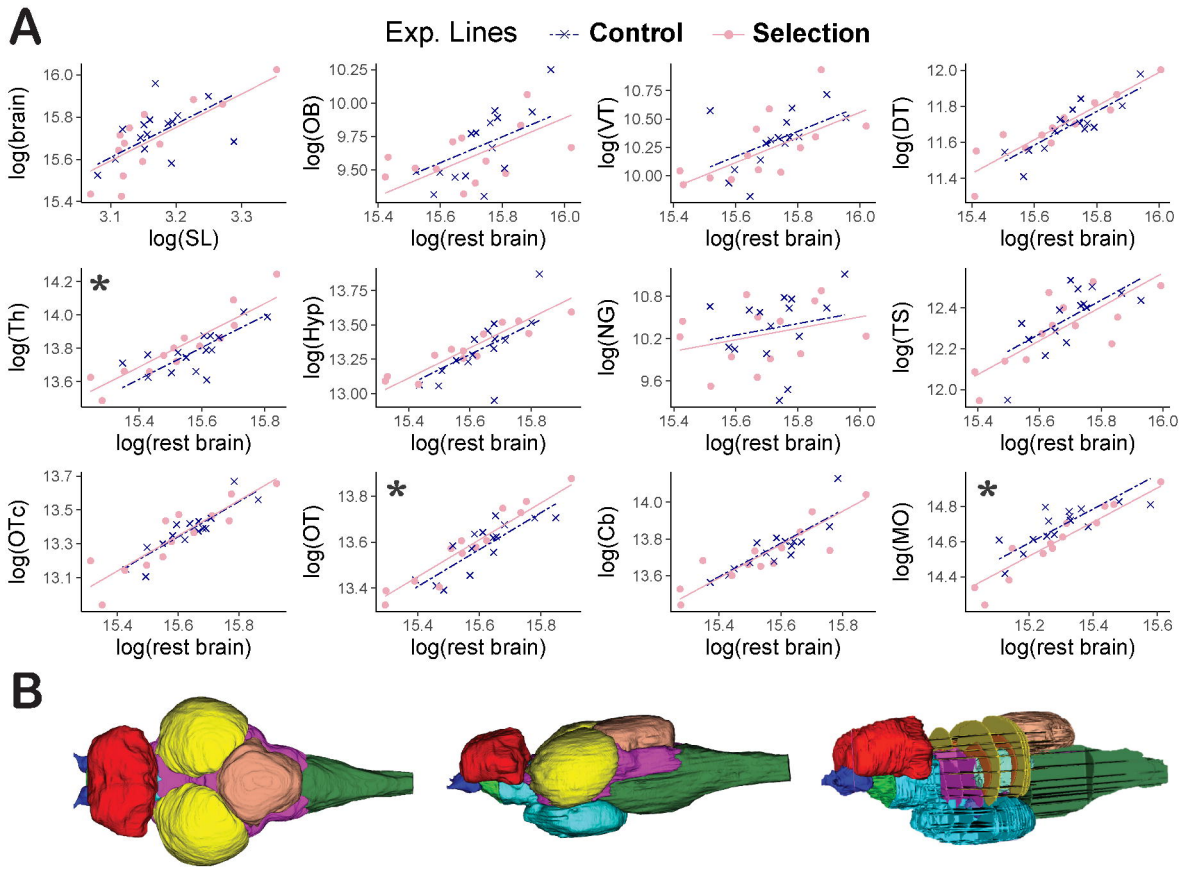
A
Exp. Lines
Control
Selection
log(brain)
log(SL)
log(OB)
log(rest brain)
log(VT)
log(rest brain)
log(DT)
log(rest brain)
log(Th)
*
log(rest brain)
log(Hyp)
log(rest brain)
log(NG)
log(rest brain)
log(TS)
log(rest brain)
log(OTc)
log(rest brain)
log(OT)
*
log(rest brain)
log(Cb)
log(rest brain)
log(MO)
*
log(rest brain)
B

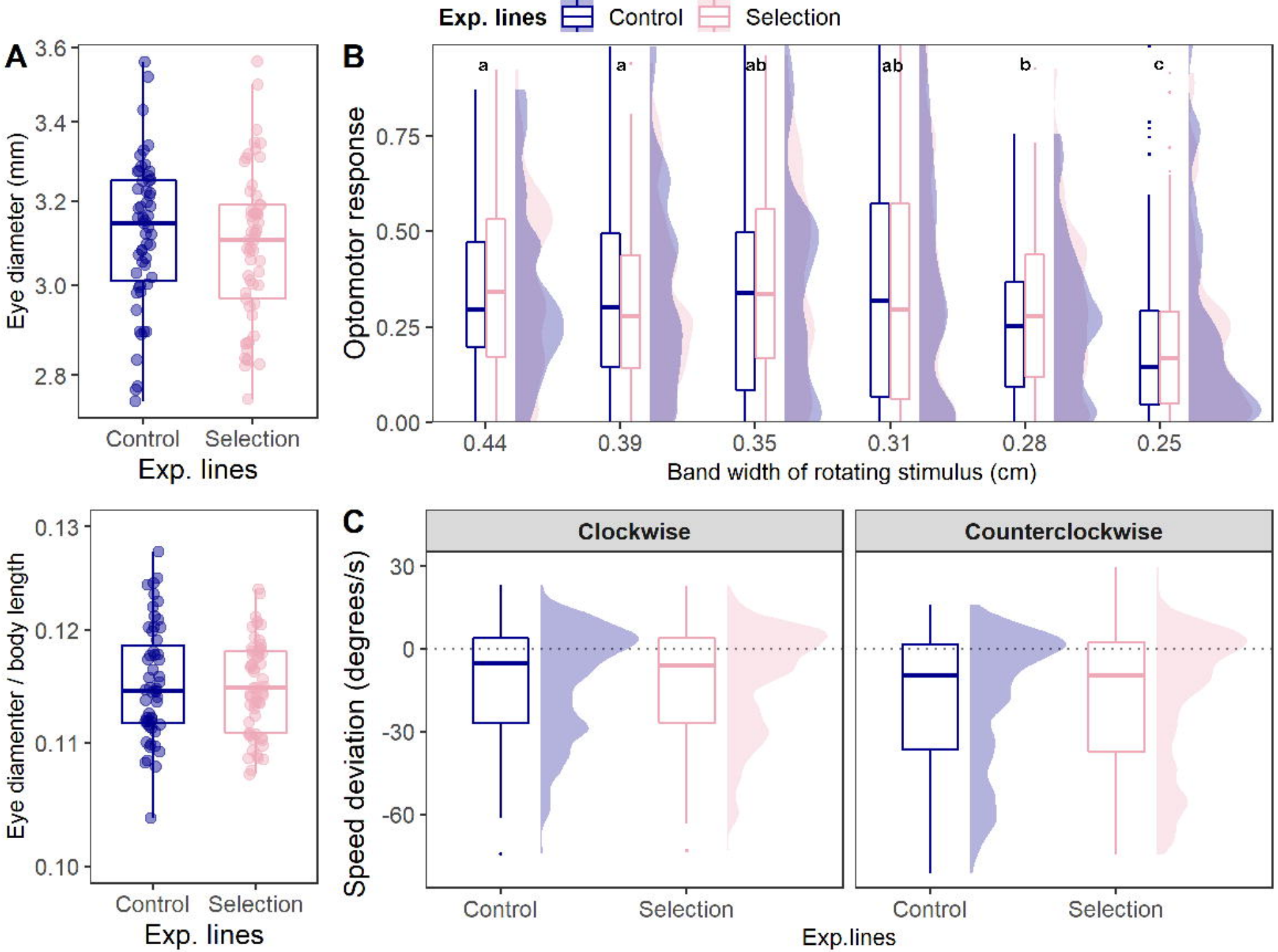
Exp. lines
Control
Selection
A
Eye diameter (mm)
3.6
3.4
3.2
3.0
2.8
Control
Selection
Exp. lines
B
Optomotor response
0.75
0.50
0.25
0.00
a
a
ab
ab
b
c
0.44
0.39
0.35
0.31
0.28
0.25
Band width of rotating stimulus (cm)
Eye diamenter / body length
0.13
0.12
0.11
0.10
Control
Selection
Exp. lines
C
Clockwise
Counterclockwise
Speed deviation (degrees/s)
30
0
-30
-60
Control
Selection
Control
Selection
Exp.lines

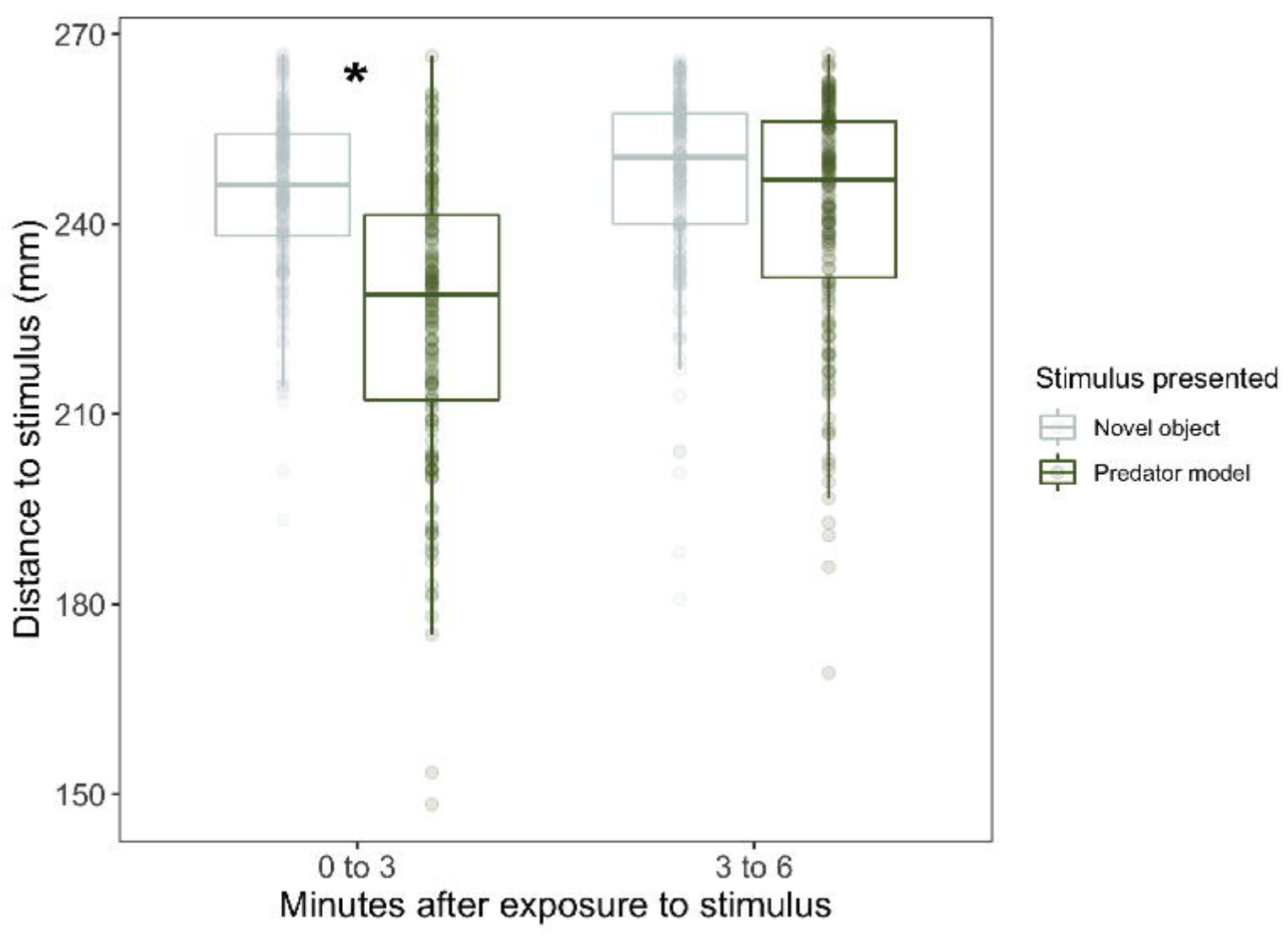
270
240
210
180
150
Distance to stimulus (mm)
*
0 to 3
3 to 6
Minutes after exposure to stimulus
Stimulus presented
Novel object
Predator model

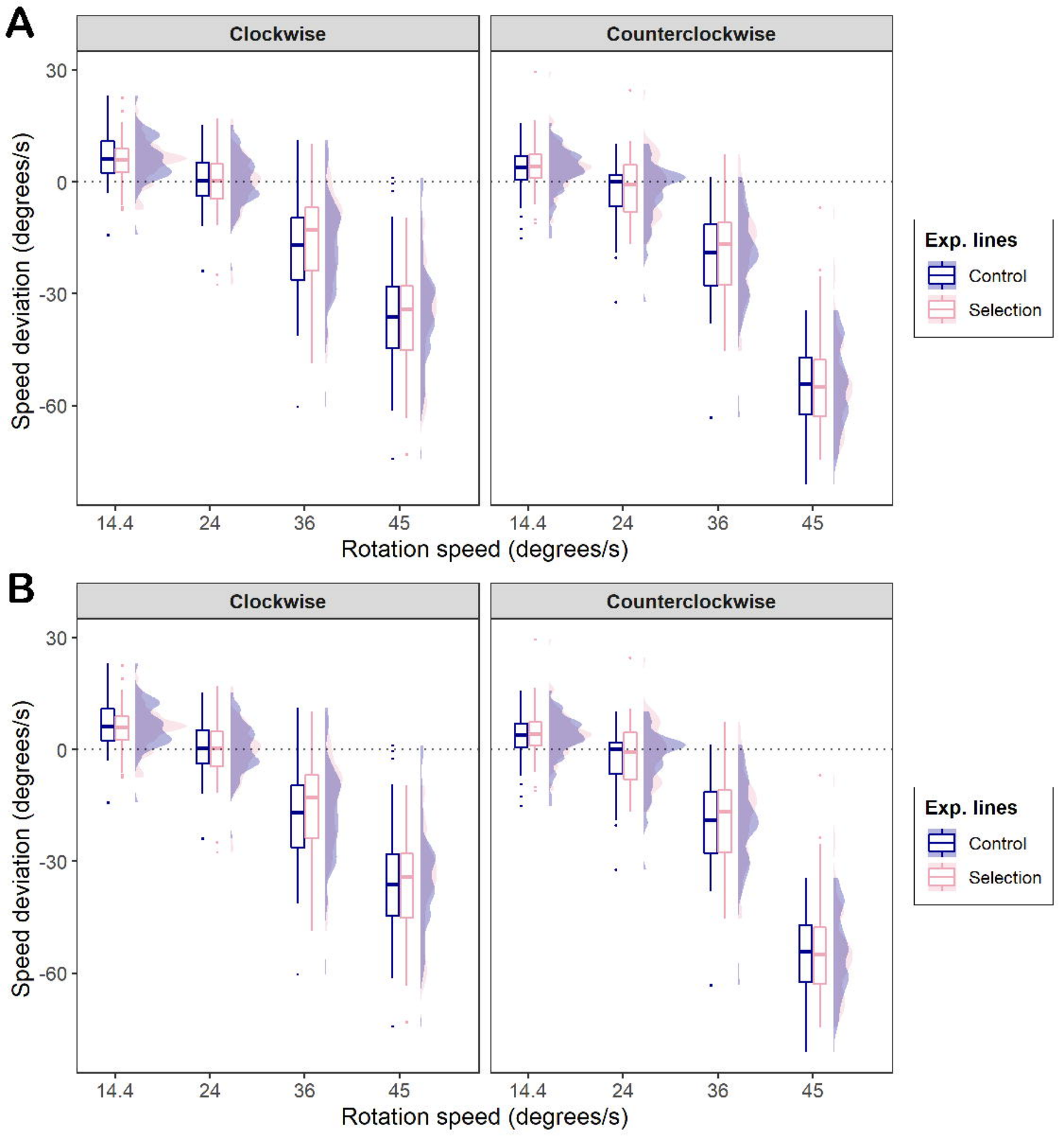
A
Clockwise
Counterclockwise
30
0
-30
-60
Speed deviation (degrees/s)
14.4
24
36
45
Rotation speed (degrees/s)
Exp. lines
Control
Selection
B
Clockwise
Counterclockwise
30
0
-30
-60
Speed deviation (degrees/s)
14.4
24
36
45
Rotation speed (degrees/s)
Exp. lines
Control
Selection